Titre: Title:	User-Oriented Demand Response for Smart Buildings
Auteur: Author:	Juan Alejandro Gomez Herrera
Date:	2017
Type:	Mémoire ou thèse / Dissertation or Thesis
Référence: Citation:	Gomez Herrera, J. A. (2017). User-Oriented Demand Response for Smart Buildings [Thèse de doctorat, École Polytechnique de Montréal]. PolyPublie. https://publications.polymtl.ca/2663/

UNIVERSITÉ DE MONTRÉAL

USER-ORIENTED DEMAND RESPONSE FOR SMART BUILDINGS

JUAN ALEJANDRO GOMEZ HERRERA
DÉPARTEMENT DE MATHÉMATIQUES ET DE GÉNIE INDUSTRIEL
ÉCOLE POLYTECHNIQUE DE MONTRÉAL

THÈSE PRÉSENTÉE EN VUE DE L'OBTENTION
DU DIPLÔME DE PHILOSOPHIÆ DOCTOR
(GÉNIE INDUSTRIEL)
JUILLET 2017

UNIVERSITÉ DE MONTRÉAL

ÉCOLE POLYTECHNIQUE DE MONTRÉAL

Cette thèse intitulée :

USER-ORIENTED DEMAND RESPONSE FOR SMART BUILDINGS

présentée par : GOMEZ HERRERA Juan Alejandro
en vue de l'obtention du diplôme de : Philosophiæ Doctor
a été dûment acceptée par le jury d'examen constitué de :

M. LE DIGABEL Sébastien, Ph. D., président
M. ANJOS Miguel F., Ph. D., membre et directeur de recherche
M. ZAREIPOUR Hamid, Ph. D., membre
M. OCHOA Luis, Ph. D., membre externe

DEDICATION

To Marie, my family and friends...

ACKNOWLEDGEMENTS

It has been a while since I left my old life to pursue a dream, to face new challenges, and to live new experiences. As this adventure draws to a conclusion, I wish to thank all those who supported me in one way or another on my journey.

First and foremost, I would like to express my sincere gratitude to my supervisor Prof. Miguel Anjos for his constant guidance, encouragement, and support. Every meeting and every piece of feedback taught me the *dos and don'ts* of being a researcher.

I thank Prof. Luce Brotcorne and the INOCS team in INRIA Lille for their hospitality during the last stage of my Ph.D., and the Mitacs Globalink program for financial support.

Thanks also to my friends and colleagues in *Team Anjos* and at GERAD for creating an amazing environment in which to laugh, learn, and improve together.

I'm grateful to my friends, Didac, Thibault, Nury, and Alvaro, who I started the Ph.D. with, and Jaime and Manuel, who came later, for sharing many special moments and for adding a family-like touch to my life.

My heartfelt appreciation goes to my family in Colombia: my parents Maria Elena and Juan Vianney and my brothers Daniel and Mauro. Your support and love through thick and thin helped to make this thesis real.

Finally, my deepest gratitude to Marie-Helene: your love and patience have made an invaluable contribution to this thesis. Love through all the stages of my journey and patience even when you didn't understand my world. I thank you from the bottom of my heart.

RÉSUMÉ

Les récents changements dans les systèmes de puissance ouvrent une frontière de défis et d'avantages potentiels pour tous les participants tout au long du réseau. Le paradigme du réseau intelligent aide à soutenir de meilleures décisions, à améliorer l'efficacité et en général à disposer d'un approvisionnement énergétique plus fiable, économique et durable. Cela accorde une importance particulière à l'intérêt croissant pour la participation des utilisateurs finaux grâce aux programmes de réponse à la demande.

Dans ce sens, la recherche présentée dans cette thèse contribue au développement et à la pénétration des programmes de réponse à la demande. Ces approches ont été conçues du point de vue de l'utilisateur, qui veut satisfaire sa demande à un coût raisonnable, mais compte tenu des variables du système de puissance telles que la réduction et le coût des pics. Pour atteindre cet équilibre, ce projet de recherche combine plusieurs éléments du monde réel et d'autres idées nouvelles afin de faire l'évolution du réseau intelligent.

L'une des principales contributions de cette thèse est l'utilisation et l'estimation des profils de capacité. Ce concept est présent dans tout le document et est particulièrement important dans les deux premières contributions. Tous les deux traitent de la détermination d'un profil de capacité adéquat. Les profils de capacité sont déterminés à l'avance et représentent les besoins énergétiques futurs des utilisateurs finaux dans un contexte de réponse à la demande.

Dans le premier cas, la méthodologie se concentre sur les appareils de chauffage et de refroidissement. Le profil de capacité fonctionne en combinaison avec un contrôleur d'admission existant pour guider l'opération de température du bâtiment. Dans cette contribution, le profil de capacité est estimé en utilisant une approche d'ajustement de données et un classificateur «multiclass ».

Dans le second cas, le cadre est conçu pour représenter des caractéristiques spécifiques d'une demande stochastique. Cette demande est générée par l'agrégation des charges basées sur l'activité dont la consommation est déclenchée par le comportement de l'utilisateur. Ici, les profils de capacité sont déterminés en fonction de l'information disponible. Tout d'abord, une approche heuristique est préconisée lorsque peu d 'informations sont connues sur les modèles de consommation des utilisateurs. Deuxièmement, une optimisation en deux étapes lorsque nous pouvons obtenir les scénarios de demande. Un élément important de cette contribution est l'inclusion d'une tarification flexible du temps et du niveau d'utilisation.

Cette politique de prix permet à l'utilisateur de déterminer le profil de capacité et ses tarifs

correspondants à partir d'un ensemble d'options fournies par le réseau. Ces tarifs personnalisés sont alignés sur le comportement normal de l'utilisateur et finalement orienter un processus d'apprentissage pour optimiser la consommation.

La troisième contribution regroupe plusieurs utilisateurs, différents programmes de réponse à la demande et diverses ressources partagées pour planifier la consommation, le déplacement de charge et la réduction de la charge pointe. Cette approche prend des informations telles que les profils de demande et les préférences des utilisateurs directement à partir des unités de logement afin de résoudre un problème d'optimisation biobjectif pour compenser la satisfaction totale des utilisateurs et le coût total de la consommation d'énergie. Cette contribution comprend une structure de coût fixe similaire à celle de la deuxième contribution pour encourager le transfert de charge.

Enfin, des expériences sont rapportées dans chaque contribution pour valider la performance de l'approche proposée. Ces résultats comprennent des éléments comme l'analyse de sensibilité, les comparaisons de référence et les fonctionnalités du monde réel afin de clarifier les points forts, les limites et les projets de recherche à venir.

ABSTRACT

The recent changes to power systems have opened up a frontier of challenges and potential benefits for all the participants. The smart grid paradigm helps to support better decisions, to improve efficiency, and to provide a more reliable, economic, and sustainable energy supply. This is particularly important given the growing interest in user participation via demand-response programs.

The research presented in this thesis contributes to the development and penetration of demand-response programs. These approaches have been developed from the user perspective, taking into account elements of the power system such as peak reduction and cost. This research combines elements from the real world and novel ideas to balance conflicting goals and move forward in the evolution of the grid.

One of the main contributions is the use and estimation of capacity profiles. The idea behind setting a capacity profile is to establish a compromise between the expected demand and the level of service perceived by the user. The capacity profiles are determined in advance and account for the users' future energy requirements in a demand-response context.

In the first contribution (Chapter 4) the methodology focuses on heating and cooling devices. The capacity profile works in combination with an existing admission controller to guide the control of the building temperature. In this case the capacity profile is estimated by a data-fitting approach and a multiclass classifier.

In the second contribution (Chapter 5), the framework is based on specific features of a stochastic demand. This demand is generated by the aggregation of activity-based loads that are triggered by the user behavior. Here, the capacity profiles are determined as a function of the available information. First, we use a heuristic approach when we have limited information about the consumption patterns. Second, we use two-stage optimization when we have the demand scenarios. One highlight of this contribution is the inclusion of a flexible time-and-level-of-use pricing. This pricing policy allows the user to determine the capacity profile and its corresponding tariffs from a set of options provided by the grid. These customized tariffs are aligned with the normal user behavior and eventually guide a learning process to optimize the consumption.

The third contribution (Chapter 6) aggregates several users, different demand response programs, and various shared resources to plan the consumption, load shifting, and peak reduction. This approach takes information such as the demand profiles and user preferences

directly from the housing units. It solves a biobjective optimization problem to find a trade-off between the total user satisfaction and the total cost of the energy consumption. This contribution includes a fixed cost structure similar to that of the second contribution to encourage load shifting.

Finally, experiments are reported in each contribution to validate the performance of the proposed approaches. We provide sensitivity analysis, benchmark comparisons, and a discussion of real-world features to help clarify the strengths, limitations, and possibilities for future research.

TABLE OF CONTENTS

LIST OF TABLES

LIST OF FIGURES

LIST OF SYMBOLS AND ABBREVIATIONS

CPP	Critical peak pricing
DR	Demand response
DSM	Demand side management
EV	Electric vehicle
EWH	Electric water heater
ISO	Independent system operator
NN	Neural networks
PLAV	Polynomial function fitted with least absolute value
PLSV	Polynomial function fitted with least squares value
RTP	Real-time pricing
SG	Smart grid
SLAV	Sigmoid function fitted with least absolute value
SLSV	Sigmoid function fitted with least squares value
TBR	Time-based rate
TLOU	Time and level of use
TOU	Time of use

CHAPTER 1 INTRODUCTION

1.1 Context

Energy, and specifically electricity, is a key resource for the current and future development of society. New technologies have facilitated many daily tasks thanks to a continuous, reliable, and secure supply of power.

The electricity business has some special characteristics that distinguish it from other industrial sectors. Electrical generation occurs in real time, so utilities and operators have to follow demand, satisfying customer needs while ensuring system stability. This can be a challenge during load peaks and congestion periods. Increasing the number of generators with a low marginal cost, such as base-load or load-following power plants, can lead to high investment and idle resources during off-peak hours. When the projected demand is close to or greater than the maximum power capacity, operators/utilities use peaking power plants (which have a high marginal cost) or import power from other nodes in the interconnected system, trying to avoid a supply–demand imbalance that could lead to system failure.

Given these conditions, consumers are important in grid decisions since reducing demand is an option when the marginal cost is too high or no more power is available. Currently some utilities and independent system operators (ISOs) offer programs to promote the use of more efficient appliances and buildings in an effort to reduce total consumption; other suppliers manage peaks by load shedding to ensure system stability, leading to lost sales and customer dissatisfaction. A third possibility is to encourage consumers' active participation through demand response (DR) programs. DR is defined as changes in consumers' normal electrical usage profile in response to incentives designed to induce lower loads.

The flexibility that DR brings to the system can go beyond peak control. In general terms, DR seeks to reduce the variability over time of the generation carried out by utilities. Thus, it facilitates the integration of distributed intermittent renewable resources such as wind and solar. These resources account for part of the total demand and therefore affect the supply–demand balance.

Currently, DR programs target residential, commercial, and industrial users. According to FERC (2012), these programs can be classified into two main groups: programs that offer load reduction contracts between suppliers and customers, and pricing programs to encourage customers to shift their larger loads to off-peak periods.

Traditionally, most of the DR potential has come from industrial customers since they repre-

sent a large consumption for a small number of participants. This facilitates the coordination of resources and increases the impact of the DR measures. The task is more challenging for the residential and commercial sectors, where the average individual consumption is low. However, these sectors combined represent 60% to 70% of the total worldwide consumption (EIA, 2016).

Intuitively, allowing utilities to take direct control of the customer appliances/loads would ensure system reliability and cost efficiency. However, this strategy may neglect user preferences and/or lead to a complex coordination problem. Allowing consumers to manage their own consumption seems a feasible way to avoid these difficulties. However, this autonomy must be aligned with the utility's interests and system stability.

Such a strategy can be considered thanks to the evolution of traditional power systems into smart grids (SG). SGs support communication among all the entities connected to the grid. Additionally, the development of tools to handle and analyze the data will support better decisions for the grid and the users. In this scenario, DR can achieve its full potential.

SG end-users have, besides a two-way information flow with the grid, other resources at their disposal. Smart appliances are able to gather data and to respond to the central controller, storage units, and distributed generation. They can help to satisfy energy requirements and even give users the ability to trade their own generation. A housing unit with these features is commonly referred to as a smart home, or more generally as a smart building.

1.2 Definition of the Problem

In this paradigm the users face new challenges and require new decision-support approaches to achieve their goals of unlimited available power at the lowest possible cost. These goals conflict, so we must find a trade-off. Current DR programs try to link the price variations (or incentives) with the users' priorities. A high priority might justify a high price in the current time frame, and low priorities could be delayed if a pre-agreed incentive were offered. The price variations usually reflect issues such as congestion and generation efficiency, allowing the users to indirectly consider the state of the grid in their decisions. In this situation, users can manage their own consumption profiles, balancing costs with the need for power.

Another way to trade-off users and grid requirements is through the implementation of capacity profiles. A capacity profile establishes a power limit over a defined period of time, providing the users with the energy requirements to perform their normal activities while encouraging peak reduction through load shifting and/or differential tariffs. These *normal* activities can vary depending on the user, the type of load or appliance, and the time of day.

The idea behind setting a capacity profile is to establish a compromise between the expected demand and the level of service perceived by the user. A low profile will decrease user satisfaction, and a high profile will not contribute to the grid priorities. A profile that provides a balance is key for the expansion of DR programs.

The estimation of a capacity profile is related to the type of load or appliance that is generating the demand. Two categories cover many of the types of loads present in the residential and commercial sectors. First, thermal loads, such as space heaters and air conditioners, operate continuously and are triggered by factors such as the external temperature. In Canada, space heaters account for around 60% of a building's energy consumption (StatCan, 2013). Second, activity loads directly relate to the activities being carried out by the users, either at home or at the office. This consumption basically maps the user behavior.

There are different ways to actively participate in DR. Giving control to a single user may have benefits for that person, but it will not make a noticeable difference to the utility's performance. Therefore, it is necessary to aggregate multiple users and to introduce electricity generation and energy storage. The aggregation, commonly known as a microgrid, consolidates the load profiles of all the users, and introduces enough DR potential to contribute to the grid performance. In this thesis the microgrid is represented by a smart building composed of several housing units, an array of solar panels, and a battery.

This higher level requires a plan that ensures demand satisfaction for each user, the best utilization of the available resources, and active participation in DR programs.

1.3 Objectives

The general objective is to provide a set of approaches to enhance DR participation in the residential and commercial sectors, ensuring user satisfaction while taking into account the grid performance. This objective is divided into three specific objectives corresponding to each of the contributions of this research:

- Develop a method to determine capacity profiles for space heating and cooling that considers the continuous and predictable operation of this type of load.
- Develop a method to determine capacity profiles for activity-based loads that considers the variability of the user behavior.
- Build a planning tool that satisfies the individual energy demands and coordinates the resources to provide DR at an aggregated level.

This is a bottom-up approach. The first two objectives deal with local decisions at the user level. In both cases the user determines the capacity profile as a function of comfort and cost. The third objective focuses on a building-aggregated level that considers multiple users. These decisions are made by a central planning module that takes into account the user preferences and the building's solar panels and storage.

CHAPTER 2 LITERATURE REVIEW

This chapter presents the most relevant literature. We first discuss articles that directly contribute to the management and optimization of the consumption on the demand side. We then present work related to load estimation and load forecasting; these are valuable tools that guide decision-making and help determine the transition between lower and higher levels in the grid. We next explore the models that characterize and include user behavior in the grid decisions, before discussing models that focus on the planning and operation of an aggregated level. We end with a discussion of the most common DR programs available and related work. Researchers in this field use a range of operations research, machine learning, and control approaches.

2.1 Demand-side Management

Various techniques have been used to manage the load on the user side. The user preferences are typically hard constraints, and the objective is to optimize the energy consumption or the peak reduction.

Esther and Kumar (2016) present a comprehensive survey of optimization-based approaches. They compare the system granularity, the type of demand (deterministic or stochastic), and the time scale.

Nguyen and Aiello (2013) discuss the importance of a consumption-aware user. This survey includes potential energy savings, activities with higher potential impact, and the availability of information and automation in the building. Soares et al. (2014) characterize the controllable demand and its potential savings for users participating in an energy management system.

A DSM strategy for a load shifting problem is presented by Logenthiran et al. (2012), using an evolutionary algorithm to minimize the difference between the proposed consumption profile and the actual observed load. It includes a set of controllable appliances for residential, commercial, and industrial users. Costanzo et al. (2012) propose an architecture based on optimal control that includes a high level to communicate with the grid through price signals; an intermediate level to obtain an optimal plan based on real and forecast information for a larger horizon; and a low level to respond to variations and to close the loop, feeding back to the upper levels. Simulation results are presented for the low and intermediate levels.

Lujano-Rojas et al. (2012) propose an optimal strategy for managing load based on forecasting

electricity prices, energy demand, and the use of electric vehicles (EVs). They start with an algorithm to determine the possible demand curve of a given appliance or EV and then solve a maximization problem driven by the difference between the value perceived by the user and the cost of power. They include two scenarios: the first determines the best time to use the EV and the second introduces a specific time frame for the use of the EV.

Load scheduling is an effective way to manage consumption. Moon and Lee (2016) present a mixed integer nonlinear model to determine the operation time and the power consumption level of each device, maximizing the difference between a utility and a cost function.

Chen et al. (2012) use stochastic and robust optimization approaches to determine the optimal schedule for a set of appliances. They minimize the expected electricity payment at the end of the day, taking into account some financial risks associated with price uncertainties. Both methods give a better cost performance than a flat price strategy. The robust method has better computational efficiency but fewer cost benefits than the stochastic approach.

Rastegar et al. (2016) propose an approach that considers priorities for the operation of the appliances. These priorities are considered in a mixed integer program that minimizes the cost for the user in a day-ahead context.

To give more flexibility to balanced generation, electric water heaters (EWH) may be considered a DR resource. Diao et al. (2012) model residential EWH under several control strategies: centralized control to provide balanced service and two decentralized approaches. The first switches off the EWHs when the local bus frequency drops below a threshold, and the second reduces the temperature of the EWHs proportionally to compensate for frequency variations.

Fernandes et al. (2014) propose a method with dynamic load priority that allows the smart home to participate in DR events. An optimization algorithm minimizes the impact of the curtailments.

2.1.1 Role of Capacity Profile

Fixing the power limit is common in DSM approaches. This encourages load shifting and demand shaping, and it guarantees a peak-control policy. This idea is explored in this thesis through the concept of a capacity profile. A capacity profile is a pre-established consumption limit that varies over time. This limit represents a trade-off between the users' power requirements and the grid's demand management priorities. An effective capacity profile will provide the users with sufficient power while avoiding unwanted peaks of demand.

In some cases a higher-level entity (utility, operator, aggregator) imposes this capacity limit.

Margellos and Oren (2016) present a framework where a DR aggregator defines a capacity constraint and the user minimizes costs by solving a stochastic program. They also explore increasing the capacity levels, provide bidding curves, and analyze price sensitivity.

The approach introduced by Caprino et al. (2014) allows the activation of one load at a time. The peak of consumption is bounded by the load with the largest power requirement. Rahim et al. (2016) define the DSM problem as a knapsack problem with preset capacities; they evaluate the performance of several heuristic-based controllers. Ogunjuyigbe et al. (2017) present a variation of the capacity limit through the inclusion of a predefined budget and a user-expenditure and satisfaction ratio; the users seek to maximize their satisfaction.

Li et al. (2016) determine the optimal allocation of capacities using a queueing strategy. The service provider determines the capacity to assign to each user from a set of renewable resources and demand requests. In a similar way, Doorman (2005) explores capacity subscription where the users compete for limited power resources.

These works utilize capacity profiles intended to contribute to the grid performance. Although some user preferences are considered, the users do not make decisions about their power and energy requirements. How to determine a capacity limit that provides benefits for both grid and user is an open question.

2.2 Load Forecasting

DSM approaches normally use capacity limits that were previously computed. The performance of a capacity profile is directly related to the demand and the expected level of user satisfaction. In this section we explore tools used to estimate the power consumption. This is a key step for both consumers and utilities. The users can guide their DSM modules, and the utilities can gather valuable information about the global performance of the system.

Relevant publications can be found in the load-estimation literature. Swan and Ugursal (2009) give the general structure of this type of problem. Their comprehensive review classifies the estimation or forecasting approach depending on the level of aggregation of the input data. These can be bottom-up models, which extrapolate the behavior of a large system based on its components, or top-down models, which make top-level decisions and share the output among all the subsystems.

Suganthi and Samuel (2012) review the most frequently used methods for forecasting. They consider classical time series, other statistical approaches, and sophisticated machine-learning tools. Many of these methods have been used to estimate energy demand.

Jain et al. (2014) use support vector regression to forecast consumption in residential build-

ings. They evaluate the impact of the time (daily, hourly, 10 min) and space (building, floor, unit) granularity inside a multifamily unit. The best coefficient of variation is achieved in the combination (hourly, floor). The approach was applied to an empirical data set from a real building.

Al-Wakeel et al. (2017) estimate load via a k-means-based approach in a scenario with incomplete information from past consumption. Massana et al. (2015) consider buildings with daily or seasonal patterns and present a short-term forecasting method for aggregated loads.

A comparison of artificial neural networks and the auto-regressive integrated moving average is presented by Ahmed et al. (2014), showing the effect on the scheduling of storage devices.

Mohajeryami et al. (2017) highlight the importance of accurate estimation for exploiting DR potential. Specifically, they present an error analysis for different load estimation tools that are used in real-world operations.

The above articles have something in common: the forecast load is a continuous value. If the prediction output belongs to a discrete set of classes or categories, the estimation problem can be defined as a classification problem. Such problems are common in the context of power systems but less common for estimating future loads. Zareipour et al. (2011a) forecast prices that are above or below a specified set of thresholds, and Zareipour et al. (2011b) forecast the severity of wind power ramp events. Both approaches are based on support vector machines.

2.2.1 Bottom-up User-Oriented Load Estimation Models

DSM approaches generally consider user requirements such as preferred time windows, earliest and latest starting times of the appliances, and user comfort. It is assumed that the user behavior will match the optimal consumption plan. Some work focuses on understanding and characterizing the behavior of the users in residential and commercial buildings. This leads to a more realistic representation of a consumption profile. Typically, this profile is obtained from the aggregation of the individual loads generated by the activities that the users carry out regularly.

Richardson et al. (2010) present a model that determines consumption profiles based on the aggregation of individual loads, the number of people in the housing unit, and their activity profiles. In a similar way, Collin et al. (2014) use a Markov-chain Monte–Carlo model to compute the activity profiles and estimate realistic load profiles for a wide variety of housing units. A highlight of this work is the software *Desimax* that generates activity and consumption profiles based on information from government databases.

Subbiah et al. (2013) perform logistic and Poisson regression to estimate energy demand in a large aggregated population. They model the correlational and consistency elements of the shared activities of multiple inhabitants in a household. Similarly, Munkhammar et al. (2014) estimate consumption profiles for single and multiple housing units by fitting probability density distributions over a historical set.

All these estimation tools provide the decision-maker with information about electricity consumption over time. This idea can be extended to determine the capacity profile that will account for this expected demand while providing DR and ensuring the user's minimum power requirements.

2.3 Aggregation

Typically, when we talk about aggregating end-users into a single entity in the presence of storage and/or distributed generation, we refer to a microgrid. Parhizi et al. (2015) present a comprehensive review of microgrids, including investment, operation, generation technologies, communication requirements, and grid-support capabilities.

Some works focus specifically on the planning and control of the system. Parisio et al. (2014) control the operation of a microgrid in a realistic scenario. They use a model predictive control strategy to schedule the generators, storage devices, and controllable loads, while compensating for the uncertainties in the dynamics of the system.

Kriett and Salani (2012) introduce a similar approach, focusing on models for combined heat and power generation in the presence of thermal and electrical loads and storage units. Mhanna et al. (2016) aggregate different types of appliances and distributed energy systems to schedule loads for large populations. Palma-Behnke et al. (2013) perform an economic comparison of a rolling-horizon approach and the standard unit commitment for microgrids.

Mixed integer programs have been used to determine how to integrate the microgrids into the distribution system. Mesari and Krajcar (2015) and AlSkaif et al. (2017) encourage the use of the batteries of EVs and the available renewable resources by minimizing the use of conventional resources. Their goal is to ensure a high level of self-consumption.

Chabaud et al. (2015) assess several configurations of a grid-connected microgrid, considering a two-way flow of power and its impact on the grid. Detroja (2016) considers the generation and consumption sides and the balance between the two in a real-time scenario for the optimal operation of an autonomous microgrid.

2.3.1 Multiobjective Approaches

As mentioned previously, the user perspective is typically represented by elements such as preference constraints and/or costs that approximate the level of satisfaction while minimizing the total operational cost. Multiobjective optimization can enhance the user's participation in the decision process. It finds a trade-off between conflicting objectives such as cost and comfort.

When objectives conflict there is no solution that optimizes them simultaneously. To improve one of the objectives we need to worsen one or more of the others. The best solution is said to be nondominated, Pareto efficient, or Pareto optimal (Ehrgott, 2006). Marler and Arora (2004) provide a comprehensive review of methods for finding Pareto-efficient solutions. They present approaches that include the user preferences in the decision-making and that represent and approximate the Pareto front (the set of Pareto-efficient solutions).

For power systems and SGs, multiobjective optimization has been used in various ways. Sometimes the decision makers are interested in finding a good representation of the Pareto front. Yang and Wang (2012) use particle swarm optimization and weighted aggregation to approximate the Pareto front for energy cost and environmental comfort.

The ϵ-constraint method is often used to approximate Pareto fronts. Zhang et al. (2012) use this approach to balance the total cost and the energy obtained from distributed generators in isolated sites, and Hosseinnezhad et al. (2016) and Aghaei and Alizadeh (2013) use it to minimize both pollutant emission and operating cost.

Sometimes the decision-maker looks for a single efficient solution. Cao et al. (2017) and Korkas et al. (2016) use a weighted-sum approach to reduce the conflicting objectives to a single objective. The former authors balance the minimization of load curtailment, operating cost, and pollutant emission. The latter authors deal with the energy costs and thermal comfort.

Finally, Choobineh and Mohagheghi (2016) implement a lexicographic goal programming method to minimize the operational costs, the emissions produced, and the asset deterioration resulting from exposure to extreme temperatures.

Typically, aggregation approaches explore the technical and operational aspects of the system, whereas multiobjective methods explore the trade-off decisions in an aggregated system. A more comprehensive approach would integrate the operational aspects and the conflicting objectives with the impact on the individual users of the system.

2.4 DR Programs

In smart buildings the interaction with the utility is driven by DR programs. Such programs are a trending topic, and their presence is increasing (about 9.2% of U.S. peak demand (FERC, 2012)), but the idea of planning the demand of electric systems was introduced several decades ago. An initial and still valid classification of load-shape goals was presented by Gellings (1985). These include direct shedding to avoid peaks, load shifting from peak to off-peak periods, and other strategic decisions such as conservation or growth.

The DR concept was introduced to target these goals. Although some strategies have been used in electricity supply management for decades, DR combines them, adds new possibilities, and takes the planning to the next level, introducing technological issues and the active participation of customers in the decision-making process. It changes the unidirectional information flow into two-way communication and aims to ensure system reliability and company profitability. According to Walawalkar et al. (2010), a large reduction in the marginal cost of production may be achieved through a small reduction in demand.

DR strategies can be classified into two main groups (FERC, 2012). First, incentive-based programs respond to critical peaks by a reduction contract between power suppliers and customers. Such contracts allow the utility to reduce the supply of electricity for a given period. The utility may be able to remotely shut off user loads at short notice. The customers may commit to a prespecified reduction, earning compensation and facing penalties if the reduction is not achieved. Other programs provide incentives for voluntary reductions without penalties. Most of these programs are oriented to industrial and commercial businesses. However, a smart building aggregates enough residential/commercial load to have a potential impact on the load-shaping.

Second, time-based rate (TBR) programs encourage customers to move larger loads to off-peak periods (load shifting). These programs are based on historical information or on real-time data. The pricing policies range from a basic time-frame structure to a more complex but accurate system. The most common policies are time of use (TOU), critical peak pricing (CPP), and real-time pricing (RTP). TOU programs have different prices for on-peak and off-peak periods. CPP programs add real-time pricing during extreme system peaks where the traditional peak/off-peak structure is not enough; usually the critical-peak price is much higher than a normal peak price. Finally, RTP programs link the hourly prices to hourly changes in the day-of (real-time) or day-ahead cost of generation. In this thesis we explore the combination of TOU with the previously introduced capacity profile. There are two sets of tariffs, one for consumption below the limit and one for consumption that exceeds the limit.

The time and level of use (TLOU) pricing keeps the original structure of time-dependent prices but allows a more flexible pricing strategy for users and utilities.

Pricing policies that consider power-peak-related penalties are currently offered to large industrial customers. In Quebec, the *rate L* provides a tariff for the energy consumption and a tariff for the peak demand (Hydro-Quebec, 2017). For the residential sector, the national service in Italy offers contracts with a maximum constant power limit; no consumption above that limit is allowed (SEN, 2017).

The best policy for the supplier depends on its demand curve and the integration of SG elements to facilitate communication. Muratori and Rizzoni (2016) and Vardakas et al. (2015) assess various pricing policies to explore the effect on user participation and grid performance. A pricing policy that considers user behavior facilitates the integration of the user into the SG decisions. The price setting problem is presented by Afsar et al. (2016); they use a bilevel optimization approach to find a trade-off between the revenue obtained by the energy provider and the user dissatisfaction. The use of declining block rates is explored by Hasib et al. (2015) to achieve a balance between user comfort and electricity cost. They present a microeconomic analysis of this function, and the method is used for bidirectional energy trading.

Walawalkar et al. (2010) and Cappers et al. (2010) give surveys of DR performance and resources. Walawalkar et al. (2010) include a classification based on the activating event, such as emergency and economic programs. Emergency programs seek resources to cope with congestion and to avoid system outages. Economic programs help to balance the market and the electricity price, and ancillary service programs offer frequency regulation and operating reserves.

Trading structures have been changing in recent decades from a vertical integrated approach to an open multi-player structure. These new schemes seek more efficient performance throughout the supply chain, reducing unnecessary costs and investments and introducing competition. This has led to new opportunities for DR programs. Initially, utilities/generators offered DR programs in a direct bilateral agreement with consumers, but the new market rules have changed this. Third-party entities have started to offer DR programs, buying load reduction capability and selling it to the load-serving entity (utility/ISO). Market-based DR programs have given consumers the ability to bid for specific load reduction or an ancillary service. These conditions bring benefits in terms of market performance, increased options for customers, and reduced price volatility.

CHAPTER 3 THESIS ORGANIZATION

Several factors link the contributions of this thesis. Some of them establish connections between the articles, and others highlight the differences and open a frontier of future extensions. The user perspective is at the core of this research, and it is a component of all the contributions. The user perspective is considered through three main elements: demand satisfaction or quality of service, total cost, and capacity profile. The capacity profile is used to keep track of the grid requirements while considering the user preferences.

The first contribution (Chapter 4) focuses on the estimation of capacity profiles for the operation of space heaters and cooling systems for smart buildings. This approach works with an existing admission-control module that manages the loads in real time. The admission controller achieves a shaving effect on the demand curve by using a user-defined capacity limit. We seek a capacity profile that ensures user comfort and is able to provide peak control. We capture specific features of this type of load: continuous operation over time and relative independence of most of the user's activities. We do not consider energy cost in the decision process since this type of demand was considered highly inelastic from the user perspective.

The second contribution (Chapter 5) also concerns the estimation of capacity profiles, this time considering activity-based loads. This type of load is strongly influenced by user behavior, so we used a stochastic optimization model. The users buy or book capacity in advance, aiming to satisfy their energy requirements while minimizing the total cost. One of the main features of this contribution is the integration of a flexible cost structure that works together with the capacity profile. This scheme meets the user's needs and results in an economical option for many of the user's potential decisions. Demand satisfaction is always guaranteed.

The third contribution (Chapter 6) introduces the multiple-user context. This contribution determines the operational plan for a multi-unit smart building, taking into account the individual demands and willingness to shift load, and the presence of shared solar panels and shared storage. The user preferences are included in the willingness to shift and are traded-off (with cost) through a biobjective optimization problem solved via compromised programming. The model considers a cost structure similar to that of the second contribution, with tariffs and capacity limits that are preset by the utility or grid operator. This collaborative approach ensures the demand satisfaction that the user considers essential and provides peak reduction, through the combination of battery, local generation, shifted load, and pricing policy. Finally, Chapter 7 provides concluding remarks.

CHAPTER 4 ARTICLE 1: POWER CAPACITY PROFILE ESTIMATION FOR BUILDING HEATING AND COOLING IN DEMAND-SIDE MANAGEMENT

Authors: Juan A. Gomez, Miguel F. Anjos.
Published: Applied Energy, Volume 191, 2017

Abstract

This paper presents a new methodology for the estimation of power capacity profiles for smart buildings. The capacity profile can be used within a demand-side management system in order to guide the building temperature operation. It provides a trade-off between the quality of service perceived by the end user and the requirements from the grid in a demand-response context. We use a data-fitting approach and a multiclass classifier to compute the required profile to run a set of electric heating and cooling units via an admission control module. Simulation results validate the performance of the proposed methodology under various conditions, and we compare our approach with neural networks in a real-world-based scenario.

Keywords

Smart buildings, power demand, residential load sector, least squares, parameter estimation, classification.

4.1 Introduction

In the context of power systems, reducing peaks and the fluctuation of consumption brings stability to the system and benefits to the players in the power supply network. In this respect, demand-response (DR) programs and demand-side management (DSM) systems encourage and facilitate the participation of the end users in the grid decisions. This participation is increasing with the development and implementation of smart buildings. DR programs have mostly been oriented to large consumers, but smart buildings can exploit the DR potential in residential and commercial buildings as well. These represent around 70% of the total energy demand in the United States (EIA, 2016). In Canada, space heating is responsible for more than 60% of the total residential energy consumption, due to the cold

climate (StatCan, 2013). Across the country, electric baseboards account for 27% of heating equipment, reaching 66% in the province of Quebec. On the other hand, the province of Ontario is typically a summer-peaking region due to the high temperatures during that season and the high penetration of air-conditioning systems (IESO, 2015; NRCan, 2011).

Several authors have published DSM-related results. Normally their research motivation is oriented to load management, user behavior, cost performance, and curve shaping. Imposing a capacity constraint is a common idea among these approaches. Costanzo et al. (2012) propose a multilayer architecture that provides a scheme for online operation and load control given a maximum consumption level. In the stochastic DSM program in Margellos and Oren (2016), a DR aggregator imposes a capacity constraint. Bidding curves and price analyses are reported in order to guide end-users about increasing capacity. Rahim et al. (2016) evaluate the performance of several heuristic-based controllers. They define the load management as a knapsack problem with preset power capacities for each time slot. In a similar way, Caprino et al. (2014) assumes a consumption limit that allows the activation of only one load at a time. Li et al. (2016) look for an optimal allocation of capacities based on a queueing strategy. The service provider determines the capacity to assign to each user from a set of renewable resources.

The idea of capacity subscription is explored in Doorman (2005), where the individual consumer's demand is limited in a competitive market. On the other hand, the heuristic algorithm proposed in Logenthiran et al. (2012) aims to minimize the error between the actual power curve and the objective load curve by moving the shiftable loads. In this case the objective load curve can be seen as a soft constraint capacity profile.

A variation of the capacity limit is presented in Ogunjuyigbe et al. (2017), where each individual user has a predefined budget to maximize his/her satisfaction.

All the approaches mentioned represent the capacity as a given parameter, and some of them recognize the importance of using a forecasting tool to determine its value. Estimating the user consumption is a key step in the decision-making process for users and for higher levels in the power system. Relevant publications can be found in the load-forecasting literature. Suganthi and Samuel (2012) give a comprehensive review of forecasting methods from classical time series to more sophisticated machine learning tools.

Load estimation methods are classified depending on the level of aggregation of the input data: they can be bottom-up or top-down (Swan and Ugursal, 2009). Bottom-up models extrapolate the behavior of a larger system based on its inner elements. Top-down models make decisions from a global perspective and share them among all the subsystems.

Notation

$h \in \{1, 2, \ldots, H\}$	Set of time frames in horizon.
$t \in \{1, 2, \ldots, S\}$	Set of time steps in time frame h (same for every h).
$i \in \{1, 2, \ldots, I\}$	Set of loads.
N_h	Number of requests received in time frame h.
P_i	Power level of load i (kW).
C_h	Power capacity in time frame h (kW).
$r_{i,t}$	$\begin{cases} 1 & \text{if a request is created by load } i \text{ in time step } t \\ 0 & \text{otherwise} \end{cases}$
$x_{i,t}$	$\begin{cases} 1 & \text{if request from } i \text{ is accepted in time step } t \\ 0 & \text{otherwise} \end{cases}$
QoS_h	Quality of service in time frame h.
$\widehat{QoS}_h$	Quality of service of the prediction model in time frame h.
T	Temperature (°C).
T_h^e	External temperature in time frame h (°C).
$\mathcal{P}$	Power levels of the loads in each scenario.
Ω	Discrete set of capacities.
$\omega \in \Omega$	Capacity class.

Within these two categories different approaches have been used to estimate the energy demand. Ahmed et al. (2014) compare artificial neural networks and the auto regressive integrated moving average, showing the effect on the scheduling of storage devices. Jain et al. (2014) use support vector regression to evaluate the impact of the time and space granularity inside a multi-family unit. Al-Wakeel et al. (2017) use a k-means-based load estimation method to compute future load profiles using complete and incomplete past information.

Logistic and Poisson regression are used in Subbiah et al. (2013) to estimate energy demand in a large aggregated population. In a similar way, Massana et al. (2015) presents a short-term forecasting method for aggregated loads, specifically in buildings with daily or seasonal patterns of consumption. Mohajeryami et al. (2017) present an error analysis for different load estimation methods that are used in real-world operations. They highlight the importance of an accurate estimation for exploiting the DR potential.

On the other hand, when the prediction output belongs to a discrete set of categories the estimation can be defined as a classification problem. Some related energy problems are

treated in this way: price forecasting in Zareipour et al. (2011a) and wind power ramp events in Zareipour et al. (2011b).

This paper proposes an approach for the estimation of a power capacity profile that works in combination with the admission controller (AC) module presented in Costanzo et al. (2012). This profile is used to ensure enough power to meet the demand for the next planning horizon (e.g., the next day in a day-ahead DR market). This novel approach takes advantage of the structure derived from the estimation problem to compute capacity profiles efficiently and reliably. Estimating the capacity that will be necessary allows us to define a relationship between the total expected demand and the level of service the user desires while providing DR. In this scenario the user will book a variable maximum power capacity per time frame over the planning horizon, ensuring a pre-established level of service. This approach could also include external factors such as peak control and pricing policies. The motivation is that a defined power *budget* limits the consumption and encourages load shifting. It also facilitates the integration of differential pricing for both energy and power.

This paper is structured as follows. We describe the proposed methodology in Section 4.2. We give simulation results for the real-world-based scenario in Section 4.3, and Section 4.4 presents our conclusions.

4.2 Power Capacity Profile

Figure 4.1 shows the application of the AC module presented in Costanzo et al. (2012). The online algorithm in the AC has four stages.

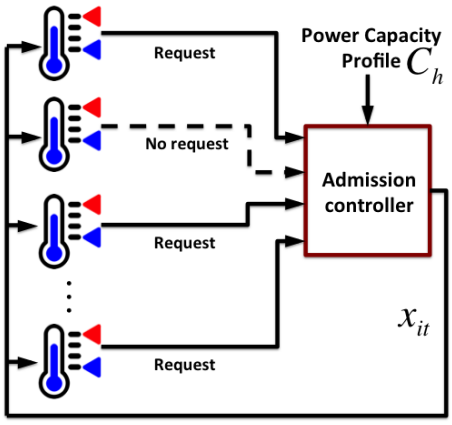

Figure 4.1 Admission controller.

First, the space heaters and the air conditioners create requests $r_{i,t}$ when the room temperature is out (or going out) of the thermal comfort zone. Second, the algorithm sorts all the

requests from the highest to the lowest priority value; the priority value is the normalized difference between the temperature in the room and the external temperature. Third, the AC accepts the highest priority requests until the given capacity C_h is consumed; the other requests are rejected. Finally, it sends the signal $x_{i,t}$ back to each smart load i either to run (if accepted) or to stand by for the next time step (if rejected).

Figure 4.2 presents a basic example of the AC operation. A smart house with two rooms, R1 and R2, is simulated over a horizon of 5 time frames. Each time frame has 10 time steps where the smart loads can send requests. Typically, a time frame would be equivalent to an hour in a realistic scenario. There is a 1.5 kW space heater in each room, and the external temperature is 5°C (Figure 4.2(a)).

We can see the peak reduction obtained by the AC in Figure 4.2(b); the end-user agrees to have a preset power capacity (dashed red line), which constrains the consumption to at most 1.5 kW. The peak of consumption, for this example 3 kW, would be attained when the two space heaters are being used at the same time step. Figures 4.2(c) and 4.2(d) show the internal temperature in each room within a certain comfort zone. In a similar way, we can see the time steps where the heaters are working in Figures 4.2(e) and 4.2(f). For more details about the AC algorithm and the heat transfer equations we refer the reader to Costanzo et al. (2012).

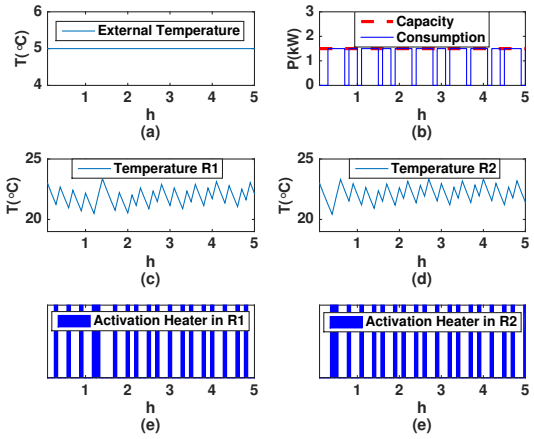

Figure 4.2 Example of results from admission controller.

In the previous example the capacity profile suffices to keep the average internal temperatures $(21.8, 22.2)°C$ in the comfort zone $[20 - 24]°C$. In the event that the temperature in a room goes out of the comfort zone during a time step, the space heater will increase its priority value, and the AC will accept the request in the next time step. The capacity profile also

achieves a peak shaving effect. However, alternating the use of the heaters might not be enough to ensure a comfortable internal temperature if the external temperature is extremely low; a higher capacity profile might be required. This decision becomes more complex if we increase the number of space heaters and if they have different power requirements.

We introduce the quality of service (QoS) index to quantify the impact of a given capacity on the whole system. The general idea of QoS is that the user should be willing to pay more if a higher level of service is desired. This decision-making by the user is especially important under time-of-use pricing conditions because the customer can profit from the cheaper time frames by reshaping the load curve while ensuring the desired QoS.

In a smart building it is possible to compute the QoS from the information provided by thermostats and smart loads connected to the AC. In the spirit of Cluwen (2014), we define the QoS for each time frame h as follows:

$$QoS_h = \begin{cases} \dfrac{\sum_{i=1}^{I} \sum_{t=1}^{S} x_{i,t}}{N_h} \times 100\% & N_h > 0 \\ 100\% & N_h = 0, \end{cases} \tag{4.1}$$

where $N_h = \sum_{i=1}^{I} \sum_{t=1}^{S} r_{i,t}$.

The accepted requests have to satisfy

$$\sum_{i=1}^{I} x_{i,t} P_i \leq C_h \qquad \forall t \in \{1, 2, \ldots, S\}. \tag{4.2}$$

Equation (4.2) indicates that the AC accepts requests until the capacity limit is reached. In the framework of this article we assume that both air-conditioning units and electric baseboard heaters have a constant level of consumption (Kuzlu et al., 2012). Let $C_h \in \Omega$, where Ω is a set of capacities that can work in combination with the AC and the set of loads. In other words, we do not want a capacity to operate a fractional number of loads in the time step t. Given that Ω is a discrete set we can define the classification problem

$$\Phi(T_h^e, QoS_h) = C_h \tag{4.3}$$

that determines $C_h \in \Omega$ for a given external temperature T_h^e and the QoS_h defined by the user. We solve this classification problem using a three-step approach: selection of the training set from historical data, function fitting, and final classification. We illustrate the steps in this section with a group of space heaters; Section 4.3 includes experimental results for both types of loads.

4.2.1 Sampling From Historical Data

The real data is obtained from the smart energy management system, which records the accepted requests, the rejections, and the evolution of the QoS over time. We simulate this historical data to understand the system dynamics and to implement a prediction model. The simulation conditions are:

- The set of heaters is composed of four identical units of 1.5 kW of consumption.
- The heat transfer is computed using the specific heat and Fourier's law formulations implemented in Costanzo et al. (2012) (see Section 4.3 for more details).
- The external temperature corresponds to the complete year 2013 (8760 hours) in the Montreal area (Climate, 2016).
- The comfort intervals for the internal temperatures are taken from the ISO 7730 standard analyzed in Olesen and Parsons (2002). For an *office category B* the intervals are $[20-24]$°C and $[23-26]$°C for heating and cooling respectively.
- C_h is randomly chosen from $\Omega = [1.5, 3.0, 4.5, 6.0]$ based on the interval of temperature; the highest capacities are not necessary during the warmer days (for example, with $T_h^e = 19$°C every value in Ω will return a QoS_h near 100%, affecting the quality of the data training set and the estimation).

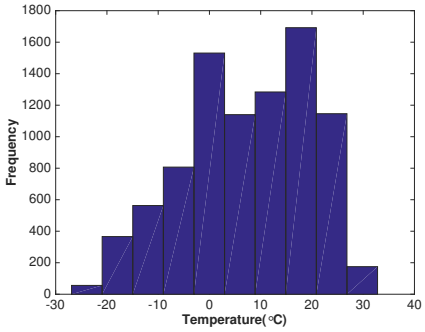

Figure 4.3 Histogram of hourly external temperatures in Montreal, Canada for 2013.

Figure 4.3 shows the frequency of the external temperature intervals in the historical data; this is clearly an imbalanced set. This imbalance is generated by the similar weather in Spring and Fall. The temperatures between 0 and 20°C would have a significantly higher weight in a fitting process. We use random under-sampling (Chawla, 2005) in order to match the number of points in the minority group from the temperatures below the comfort interval.

Figure 4.4 shows the hourly QoS results for the balanced set. We can identify several characteristics of the system behavior:

- As the temperature increases the QoS converges to higher values; with fewer requests the selection of a capacity level is a less sensitive issue.
- The selection of the capacity level has a big impact on the QoS in lower temperature conditions.
- The QoS seems to behave asymptotically for higher and lower temperatures.

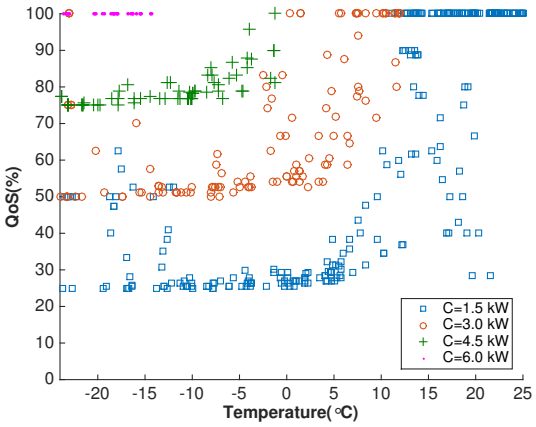

Figure 4.4 Graph of QoS vs. temperature for the sampled historical data.

4.2.2 Data Fitting

Once we have identified these features in the data set we can solve an optimization problem for the capacity estimation. We fit the sigmoid function

$$\widehat{QoS}_h = \frac{\beta_1}{1 + e^{\beta_2 T_h^e}} + \beta_3 C_h + \beta_4, \tag{4.4}$$

where $\widehat{QoS}_h$ is the quality of service from the prediction model at time frame h.

Additionally, we will compare two different optimality criteria: the least squares value (LSV) and the least absolute value (LAV). Typically, the LSV gives more weight to distant points while the LAV is resistant to outliers (Dielman, 1986).

The optimization problems are:

$$\min_{\beta_1,\beta_2,\beta_3,\beta_4} \sum_{h=1}^{H} (QoS_h - \widehat{QoS}_h)^2 \tag{4.5}$$

$$\min_{\beta_1,\beta_2,\beta_3,\beta_4} \sum_{h=1}^{H} \mid QoS_h - \widehat{QoS}_h \mid \tag{4.6}$$

Figure 4.5 shows the results for a least-squares fitting of a sigmoid function.

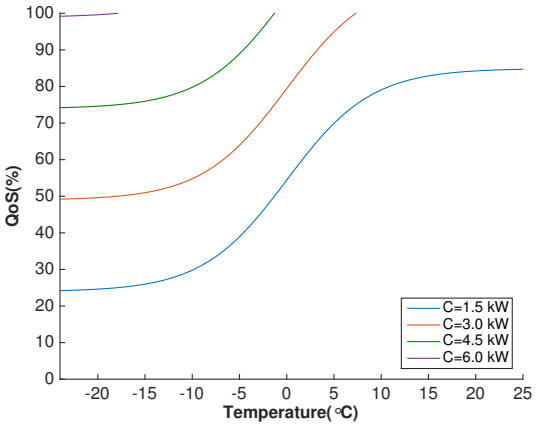

Figure 4.5 Fitted sigmoid function.

Once we have solved the optimization problem (4.5) or (4.6) we can use (4.4) to compute the expected required capacity for the desired QoS.

4.2.3 Motivation for Using a Sigmoid Function

The selection of a sigmoid function has both a graphical justification and an interesting background. We provide intuition into why it works for the heating case; the cooling case is similar. This analysis applies to any external temperature regardless of the time frame where it occurs; therefore we omit the subscript h and use N in the place of N_h to increase readability.

We make the following assumptions:

- If $T^{e'} < \hat{T}^e$ then $N(T^{e'}) > N(\hat{T}^e)$ for any temperatures $T^{e'}$ and $\hat{T}^e$.
- $C \in [C_{\min}, \infty)$ where $C_{\min} = \max(P_i)$.
- Each load generates at most one request per time step, and therefore the maximum number of requests per step equals I.
- There exists a temperature $\tilde{T}^e$ at which all the heaters generate requests at every time step, and therefore $N(\tilde{T}^e) = I \times S$.

Considering the worst-case scenario for any time frame in Equations (4.1) and (4.2), we have:

$$QoS(\tilde{T}^e, C_{\min}) = \frac{\sum_{i=1}^{I}\sum_{t=1}^{S} x_{i,t}}{I \times S} \tag{4.7}$$

$$\sum_{i=1}^{I} x_{i,t} P_i \leq C_{\min} \qquad \forall t \in \{1, 2, \ldots, S\} \tag{4.8}$$

Equation (4.8) allows us to accept at least one request at every time step. Therefore, the total number of accepted requests satisfies:

$$\sum_{t=1}^{S}\sum_{i=1}^{I} x_{i,t} \geq S. \tag{4.9}$$

After substituting (4.9) into (4.7) we can obtain a minimum QoS:

$$QoS(\tilde{T}^e, C_{\min}) \geq \frac{1}{I} \tag{4.10}$$

We can see similar behavior for scenarios with temperature $\dot{T}^e > \tilde{T}^e$ and $N(\dot{T}^e) < N(\tilde{T}^e)$. Let F be the minimum number of time steps where requests are received. Since each load i will request at most once per time step, we have:

$$F = \left\lceil \frac{N(\dot{T}^e)}{I} \right\rceil = \frac{N(\dot{T}^e)}{I} + \alpha, \quad 1 > \alpha \geq 0. \tag{4.11}$$

The variable F also becomes the minimum number of accepted requests due to the $C_{\min}$ in Equation (4.8). By substituting (4.11) into (4.1) we obtain:

$$QoS(\dot{T}^e, C_{\min}) = \frac{\sum_{i=1}^{I}\sum_{t=1}^{S} x_{i,t}}{N(\dot{T}^e)} \geq \frac{F}{(F-\alpha)I}. \tag{4.12}$$

When $\alpha = 0$ we get the same condition as in Equation (4.10).

A sigmoid function helps to represent the asymptotic extremes and monotonic behavior of the QoS. In the first case, we see how the QoS is bounded below in Equations (4.10) and (4.12), and it is bounded above by definition ($QoS \leq 100$). In the second case, the temperature and requests are inversely proportional (if $T^{e'} < \hat{T}^e$ then $N(T^{e'}) > N(\hat{T}^e)$), so $QoS(T^e)$ is monotonically increasing. Using a linear function would capture the monotonic condition

but not the asymptotic extremes.

For cooling systems we would change the first assumption to $T^{e'} > \hat{T}^e$, giving $N(T^{e'}) > N(\hat{T}^e)$. This leads to a similar monotonically decreasing sigmoid function over the interval of external temperature where cooling is required.

4.2.4 Classification

As stated previously, we have a discrete set of capacities that are suitable for the performance of the system. We solve for C_h in (4.4) in order to compute the continuous signal $\widehat{C_h}$. Finally, we use the multiclass classifier

$$C_h = \arg\min_{\omega \in \Omega} \mid \widehat{C_h} - \omega \mid \tag{4.13}$$

to find the required capacity.

Figure 4.6 shows the effect of the classifier; it assigns areas to each of the capacities based on the midpoints for each pair of sigmoid curves from Figure 4.5.

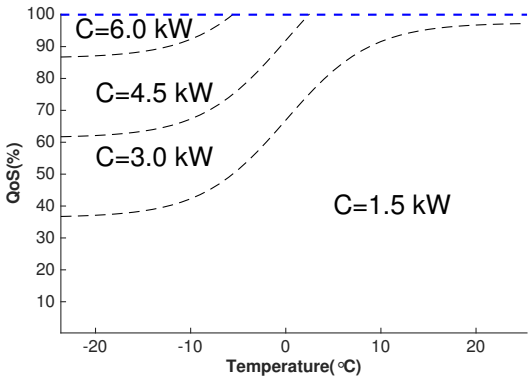

Figure 4.6 Classification areas.

4.3 Experimental Results

In the previous section we introduced the methodology with an example for a given set of homogeneous space heaters. In this section we carry out several experiments to assess and validate the performance of the proposed methodology under different conditions.

It is important to ensure coherence in the thermal system when defining the set of loads. The loads must keep the temperature in the comfort range during the warmest and coldest time frames in the data sets. This design step must include the specific features of the building

such as size, surfaces in contact with external temperatures, wall insulation materials, and thermal load inside the room. A poorly balanced thermal system could lead to a QoS of 100% with temperatures far from the comfort zone.

At the end of each time step, we compute the temperature in the rooms using the same thermal equations as in Costanzo et al. (2012):

$$\frac{dQ^{tot}}{dT^{room}} = m_{room} C_{room}, \tag{4.14}$$

$$\frac{dQ^{exch}}{dt} = -K_{wall} \frac{A}{\chi} (T^e - T^{room}), \tag{4.15}$$

$$Q^{tot} = Q^{exch} + \eta P_i, \tag{4.16}$$

where $K_{wall} = 4.8 \times 10^{-4}$ kW/m $\cdot$ °C is the average thermal conductivity of the wall, and $\eta = 100\%$ is the efficiency of the loads. We choose a room size of $60\,\mathrm{m}^3$, which corresponds to an air mass of $m_{room} = 72\,\mathrm{kg}$ with a specific heat capacity $C_{room} = 1.0\,\mathrm{kJ/Kg} \cdot$ °C. The surface area in contact with the external temperature is $A = 12\,\mathrm{m}^2$ with a thickness of $\chi = 0.2\,\mathrm{m}$. This remains constant for all the experiments.

For a more realistic scenario both types of loads are managed by the AC; the space heaters and the air conditioners will create requests when the temperature in each room is moving out of the comfort zone.

The experiments include:

- Sets $\mathcal{P}$ with homogeneous and heterogeneous power P_i values.
- Three different types of Ω sets: computed from all possible combinations of values in $\mathcal{P}$; computed from some of the combinations in $\mathcal{P}$; and given by an external entity.
- Two fitted functions.
- Two optimality criteria: LAV and LSV.
- Comparison with two neural networks (NNs) with different topologies.

The experiments are carried out in two stages. In the training stage we reproduce the approach presented in Section 4.2 in order to determine the classification areas. Then in the test stage we use the classification areas to estimate the capacity profiles for given levels of the QoS. When the profiles have been computed, we run a simulation to verify the actual QoS performance.

In Sections 4.3.1 and 4.3.2 we illustrate the methodology on a three-load instance: an apartment with three rooms. In Section 4.3.3 we report results for an instance with 50 loads to demonstrate the scalability of our methodology.

4.3.1 Training for Three-Load Instance

We required two training sets: one for heaters and one for air conditioners. Each training set is defined over the corresponding interval of temperature ($T_h^e \leq 20°C$ for heaters and $T_h^e \geq 26°C$ for air conditioners) and randomly chosen as in Subsection 4.2.1. The historical sets are simulated using the hourly temperature in Montreal for the year 2013 (8760 data points).

As mentioned before, we will compare this methodology with two other approaches. In the first case, we use the polynomial function

$$\widehat{QoS}_h = \beta_1 + \beta_2 C_h + \beta_3 T_h^e + \beta_4 T_h^e C_h \tag{4.17}$$

in the fitting step. A priori the sigmoid function gives a better representation of the historical set due to its monotonically increasing behavior and the asymptotic extremes. The function in Equation (4.17) captures only the monotonic condition. To fit each function we solve a nonlinear optimization problem using the BFGS method; it finds a solution in a few seconds.

We use NNs, which are widely used in many different types of problems, as a second benchmark. For classification problems the NN typically has the same number of neurons in the output layer as the number of classes. The NN computes the probability that each input belongs to each class, and it chooses the class with maximum probability. We implemented two NNs with $A = 1$ and $B = 2$ hidden layers (5 neurons each), cross entropy as a performance measure in the learning process, and a validation subset of 30% of the points. The training time of the NNs varies between 10 and 20 seconds using scaled conjugate gradient backpropagation.

Finally, the total confusion or missclassification index measures the performance of each approach. It indicates the percentage of the total set of data that was incorrectly classified.

Tables 4.1 and 4.2 show the training results for the different scenarios and approaches. Scenarios 1–7 and 8–14 correspond to heating and cooling respectively. In scenarios 1–3 and 8–10 the loads are homogeneous and the Ω set corresponds to all possible combinations of the loads. In scenarios 4–6 and 11–13, both homogeneous and heterogeneous loads are tested with a Ω set that was defined separately from the loads. Finally, scenarios 7 and 14 contain

a heterogeneous set of loads and all possible combinations in Ω.

Table 4.1 Confusion (%) in training stage for the heating scenarios

Scenario	$\mathcal{P}$	Ω	$PLAV$	$PLSV$	$SLAV$	$SLSQ$	NN_A	NN_B
1	$[1.5, 1.5, 1.5]$	$[1.5, 3.0, 4.5]$	28.31	33.92	12.54	13.12	11.25	10.15
2	$[2.0, 2.0, 2.0]$	$[2.0, 4.0, 6.0]$	18.94	20.38	13.48	11.70	15.76	10.10
3	$[2.5, 2.5, 2.5]$	$[2.5, 5.0, 7.5]$	20.58	25.00	20.92	17.95	15.70	10.88
4	$[1.5, 1.5, 1.5]$	$[2.5, 4.0, 6.0]$	32.04	28.50	10.01	14.47	16.2	14.25
5	$[2.0, 2.0, 2.0]$	$[2.5, 4.0, 6.0]$	25.67	22.01	12.54	14.47	17.56	14.25
6	$[2.5, 2.0, 1.5]$	$[2.5, 4.0, 6.0]$	21.46	20.21	7.01	10.51	6.75	7.25
7	$[2.5, 2.0, 1.5]$	$[2.5, 3.5, 4.0, 4.5, 6.0]$	45.63	49.21	34.96	45.38	27.69	25.01

Table 4.2 Confusion (%) in training stage for the cooling scenarios

Scenario	$\mathcal{P}$	Ω	$PLAV$	$PLSV$	$SLAV$	$SLSV$	NN_A	NN_B
8	$[0.5, 0.5, 0.5]$	$[0.5, 1.0, 1.5]$	30.15	33.23	12.26	12.73	16.11	17.16
9	$[1.0, 1.0, 1.0]$	$[1.0, 2.0, 3.0]$	18.28	19.33	10.63	9.33	19.42	8.35
10	$[1.5, 1.5, 1.5]$	$[1.5, 3.0, 4.5]$	23.40	25.75	21.61	18.00	13.54	13.13
11	$[0.5, 0.5, 0.5]$	$[1.5, 2.0, 3.0]$	31.32	36.23	12.69	19.42	9.57	9.14
12	$[1.0, 1.0, 1.0]$	$[1.5, 2.0, 3.0]$	22.08	22.44	13.96	13.74	5.36	12.40
13	$[1.5, 1.0, 0.5]$	$[1.5, 2.0, 3.0]$	22.18	24.24	8.03	11.17	22.71	13.19
14	$[1.5, 1.0, 0.5]$	$[1.5, 2.0, 2.5, 3.0]$	46.53	46.84	39.19	44.61	26.84	23.38

In general, we observe a better performance in the sigmoid fitting (SLAV and SLSV) than in the polynomial cases (PLAV and PLSV). There is no clear difference in terms of the fitting criterion. The sigmoid function seems to be competitive with both NNs in the first six scenarios of each table.

As stated before, the sigmoid function provides a better representation of the structure of the problem. Figure 4.7 shows the classification areas obtained by fitting the sigmoid and polynomial functions for scenario 2. For a QoS of 90%, we see that the polynomial function gives a transition between areas either before or after the sigmoid function. If it is before, $T \in (-18, -8)$°C, we will obtain a worse QoS and lower temperatures in the rooms. If is after, $T \in (2, 8)$°C, we will have extra capacity that is not required. This lower utilization of the capacity becomes more important if the user is paying in advance for a resource that will not be used.

On the other hand, scenarios 7 and 14 are significantly different: the NNs have considerably better performance than any other approach. Looking deeper into the characteristics of these

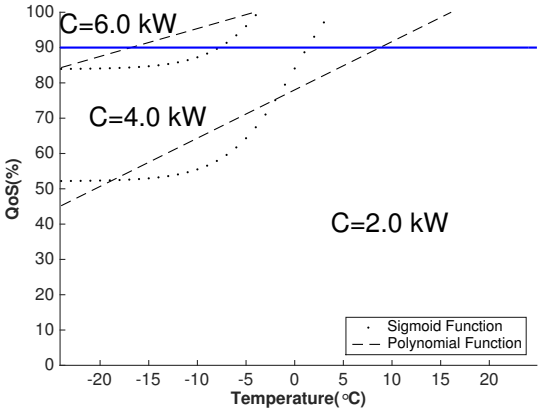

Figure 4.7 Comparison of sigmoid and polynomial areas for scenario 2.

scenarios we see a special condition: several values in Ω can generate the same QoS at the same temperature. We may have the same performance in scenario 7 for $\omega = 4$ and $\omega = 4.5$ if the three heaters send requests at the same time. In the first case, the AC will accept P_1 and P_3 and leave P_2 for the next time step. In the second case the order of acceptance changes but the QoS is the same. Figure 4.8 shows the training set for this scenario; we can see how $C = 4$ is distributed over its adjacent classes.

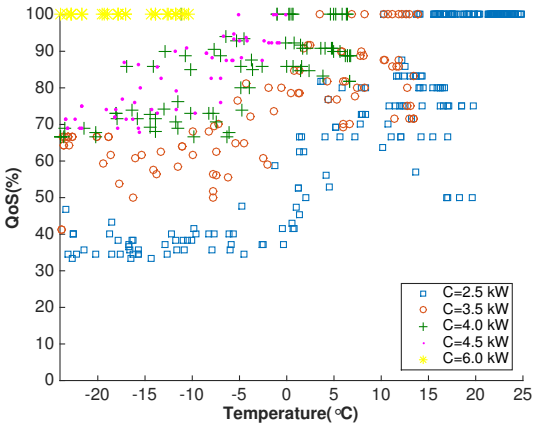

Figure 4.8 Training data for scenario 7 (heating).

Although the NNs have a better training performance, they might minimize the confusion value by eliminating one of the classes. Let W_ω be the set of points that belong to class ω, and let W_ω^1 and W_ω^0 be the subsets of points correctly and incorrectly classified respectively. Let Γ be the total number of misclassified points. The approach presented in this article separates any two contiguous sets following the fitted function, and therefore $W_1^1 + W_1^0 =\mid W_1 \mid$,

$W_2^1 + W_2^0 =\mid W_2 \mid$, and $W_1^0 + W_2^0 = \Gamma$.
If we assume that the NN eliminates class 2 we have $\bar{W}_1^1 =\mid W_1 \mid$, $\bar{W}_2^0 =\mid W_2 \mid$, and $W_2^1 + W_2^0 =\mid W_2 \mid= \bar{\Gamma}$. We can conclude that eliminating one class improves the confusion (i.e., $\bar{\Gamma} < \Gamma$) if $W_2^1 < W_1^0$.

At this point we can see the advantage of exploiting the features of the problem. In the approach presented in this paper the fitted function acts as a constraint that represents the structure of the data sets. On the other hand, the flexibility of the NNs allows a lower misclassification, but we see in Subsection 4.3.2 that this has an unexpected impact on the *QoS*.

4.3.2 Results for Three-Load Instance

The experiments use data for a period of two years (2014 and 2015) for the Montreal area (17520 data points). The user sets a *QoS* of 90%. Figures 4.9–4.14 show the results for scenarios 2 and 7 (heating) and scenario 14 (cooling). These box plots contain the minimum value, maximum value, and interquartile range for the hourly *QoS* and the hourly average temperature in the three rooms for each of the methods compared.

For scenario 2 (Figures 4.9 and 4.10) we see that the sigmoid and NN cases perform slightly better than the polynomial function. Although the *QoS* and the temperature do not vary significantly, the use of the resource differs: the polynomial function reports around 60% of utilization of capacity while the other four methods achieve a utilization between 70% and 75%. This effect was previously observed in Figure 4.7. Scenarios 1, 3 to 6, and 8 to 13 have similar results.

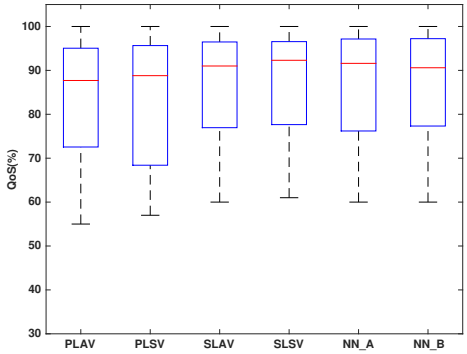

Figure 4.9 QoS test results for scenario 2 (heating).

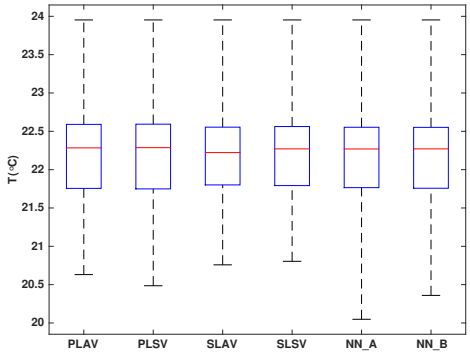

Figure 4.10 Average room temperature test results for scenario 2 (heating).

In the case of scenarios 7 and 14 we observe a special situation: although the training results for the NNs are better we have a worse QoS (Figures 4.11 and 4.13) and temperature management (Figures 4.12 and 4.14). We previously saw in Figure 4.8 that the areas for classes $3.5, 4$, and 4.5 are not clearly defined. We also saw that different capacities can result in a similar QoS at the same temperature due to the load shifting. Nevertheless, eliminating one of the classes can have negative effects on the final output; in this case the NNs tend to eliminate class 4.5 in order to minimize the confusion value. Although $C = 4.5$ and $C = 4.0$ can accept two out of the three loads if all of them arrive at the same time, the situation changes when the loads arrive at different times. For example, $C = 4.5$ will satisfy any of the combinations of two loads arriving simultaneously: $[2.0, 2.5], [1.5, 2.5]$, and $[1.5, 2.0]$, whereas $C = 4.0$ will not accept $[2.0, 2.5]$. It is therefore preferable not to eliminate a class because of the dynamics in the system.

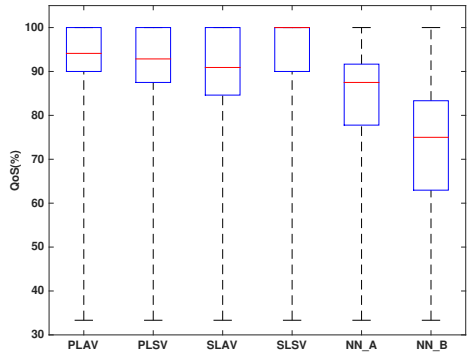

Figure 4.11 QoS test results for scenario 7 (heating).

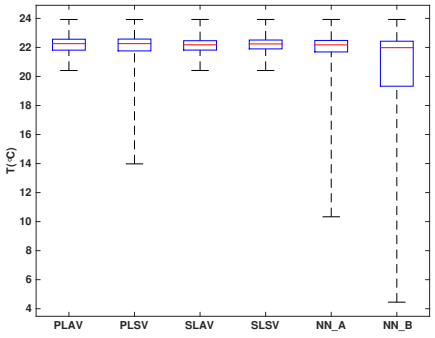

Figure 4.12 Average room temperature test results for scenario 7 (heating).

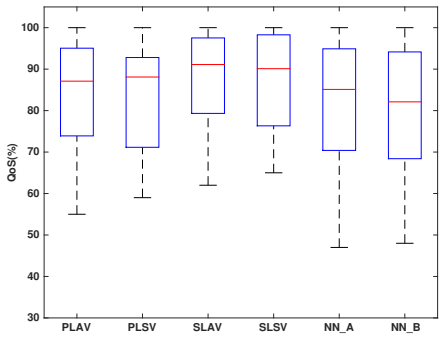

Figure 4.13 QoS test results for scenario 14 (cooling).

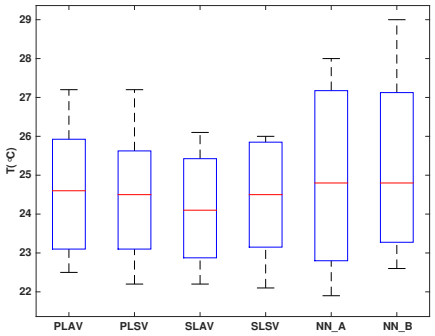

Figure 4.14 Average room temperature test results for scenario 14 (cooling).

4.3.3 Results for Fifty-Load Instance

To demonstrate the scalability of the proposed methodology, we present results for an instance with 50 space heaters. This instance represents an apartment building with three different types of heaters $\mathcal{P} = [1.5, 2.0, 2.5]$ with respectively 20, 15, and 15 loads of each type. We consider the scenario in which the building operator chooses $\Omega = [25.0, 45.0, 70.0, 90.5]$. Figures 4.15–4.17 give a summary of the results.

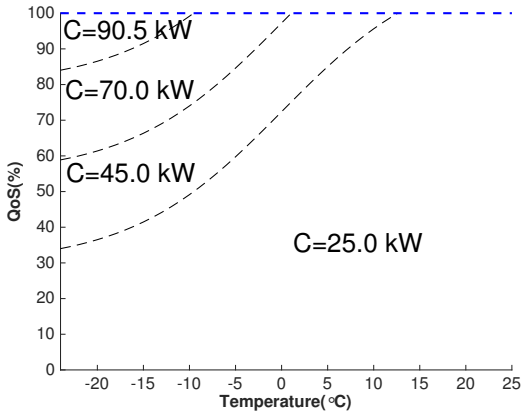

Figure 4.15 Classification areas.

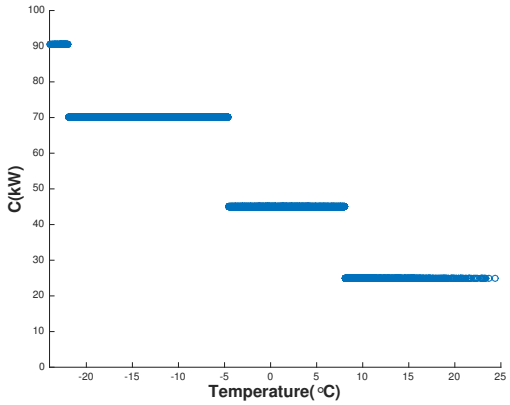

Figure 4.16 Capacity as function of external temperature.

Figure 4.15 shows that the classification areas have the expected sigmoid shape. Figure 4.16 shows that as the external temperature increases, the capacity required decreases. Finally, Figure 4.17 shows that the average QoS and the average room temperature remain in the comfort zone.

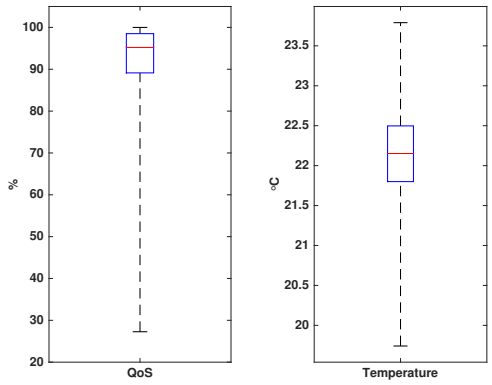

Figure 4.17 Average QoS and average room temperature.

An important feature of this novel approach is that the QoS aggregates all the requests from the loads. Therefore, regardless of the size of the population, it maintains the asymptotic and monotonic increasing behavior explained previously.

4.4 Conclusions

Understanding the requirements of residential consumption is key to facilitating increased participation in DR programs. The methodology proposed in this paper computes a power capacity profile that meets the user's expectations and at the same time provides information to residential power management systems. The use of the AC and the implementation of the QoS index allow us to aggregate a set of loads, simplifying the decision-making process.

The approach we have presented takes advantage of the inner structure of the defined problem, ensuring a good representation of the historical data and a reliable tool for future estimation. The shaving effect can be achieved, controlling the peak consumption, respecting the QoS, and ensuring a better utilization of the power capacity available.

The proposed method computes capacity profiles for a specific comfort zone with a defined set of loads. For different configurations of the building and/or different boundary conditions, the user can easily compute the new classification areas for different scenarios and intervals of comfort. The quality of the historical data and coherence in the thermal system when defining the set of loads are key to the applicability of this method.

Future work will explore the applicability of the proposed methodology to more complex systems with different types of buildings and loads and also take into account the user behavior.

Finally, the approach presented is computationally efficient, it utilizes data that is normally available in the smart building context, and it performs well for heating and cooling, offering better performance than NNs in a real-world-based scenario.

Acknowledgments

We thank the editor and the two anonymous referees for their detailed and helpful comments on earlier versions of this paper.

This research was supported by the *Canada Research Chair on Discrete Nonlinear Optimization in Engineering*.

CHAPTER 5 ARTICLE 2: POWER CAPACITY PROFILE ESTIMATION FOR ACTIVITY-BASED RESIDENTIAL LOADS

Authors: Juan A. Gomez, Miguel F. Anjos.
Submitted to Applied Energy

Abstract

This paper proposes a framework to determine day-ahead capacity profiles that account for the stochastic demand generated by user behavior in smart buildings. The user selects a level of capacity per time frame in the context of flexible time-and-level-of-use pricing. We generate the consumption scenarios by aggregating historical data. We also present two approaches to determine the required capacity given the demand. In the first approach, we solve a two-stage optimization model under the assumption that the start time probability distributions of the loads are known. In the second approach, we use a greedy-type algorithm that analyzes a set of previous consumption profiles to estimate future capacity requirements. We report experiments to validate the proposed approaches.

Keywords

Smart buildings, power demand, residential load sector, user behavior, activity-based loads, stochastic optimization.

5.1 Notation

Sets

$t \in T$	Set of time frames in horizon.
$m \in M$	Set of loads.
$i \in I$	Set of scenarios.
$j \in J$	Set of intervals of the cost step function for the lower tariff.
$q \in Q$	Set of intervals of the cost step function for the higher tariff.

Scenario Generation

P_m	Power consumption of load m (kW).
L_m	Duration of load m (h).
X_m	Start/arrival time frame of load m.
ρ	Significance threshold for the scenario elimination.

Optimization Parameters

K_t^0	TOU tariff in time frame t (¢/kWh).
K_{jt}^L	Lower tariff in interval j in time frame t (¢/kWh).
K_{qt}^H	Higher tariff in interval q in time frame t (¢/kWh).
K_t^F	Booking cost in time frame t (¢/kWh).
C_{jt}^L	Capacity lower bound in interval j in time frame t for the lower tariff (kW).
C_{qt}^H	Capacity lower bound in interval q in time frame t for the higher tariff (kW).
Pr_{it}	Probability of scenario i in time frame t.
D_{it}	Demand for scenario i in time frame t.

Optimization Variables

x_{ijt}^L	Electricity consumption at lower tariff in scenario i, time frame t, and interval j (kWh).
x_{iqt}^H	Electricity consumption at higher tariff in scenario i, time frame t, and interval q (kWh).
c_{jt}	Booked capacity in time frame t and interval j (kW).
$\bar{c}_{qt}$	Auxiliary variable to identify the higher tariff interval q in time frame t.
ϕ_{jt}	$\begin{cases} 1 & \text{Capacity in time frame } t \text{ belongs to interval } j \text{ for the lower tariff} \\ 0 & \text{Otherwise} \end{cases}$
δ_{qt}	$\begin{cases} 1 & \text{Capacity in time frame } t \text{ belongs to interval } q \text{ for the higher tariff} \\ 0 & \text{Otherwise} \end{cases}$

Heuristic

N	Number of days in Γ.
$\Gamma \in \mathbb{R}^{N \times \lvert T \rvert}$	Historical load consumption.
S	Number of time segments.
$\bar{S}(n)$	Number of time segments in iteration n.
α	Number of iterations with a constant $\bar{S}(n)$.
β	Stopping criterion.

5.2 Introduction

The increasing development of smart grids (SG) creates potential benefits and challenges for utilities, consumers, and society in general. An SG allows information flow among all the participants (Parhizi et al., 2015), supporting better decisions that ensure the stability, reliability, and economic viability of the system.

In this context, the consumers (end-users) become decision-makers and can contribute to the grid performance. This user participation is achieved through demand response (DR) programs (FERC, 2012), which are designed to encourage consumers to change their consumption preferences in a way that is beneficial for the grid, normally in exchange for compensation.

DR programs include incentive-based programs, where the consumer commits to reducing consumption over a determined period of time under prespecified conditions.

In pricing DR programs, the utility offers a variable tariff, expecting that the user will react by shifting load to cheaper periods. If the users do not shift they pay more to meet their energy requirements. These pricing policies normally reflect the aggregated peak of demand and therefore the utility's generation costs. They are mostly oriented to customers in residential and commercial sectors and have particular potential in smart buildings (Siano, 2014), where the end-users can seek to benefit while meeting the grid requirements.

The residential and commercial sectors have a specific set of characteristics that must be taken into account. First, the demand is driven by a large number of end-users with low individual consumption. Second, the consumption is triggered by the user behavior, which may be (highly) stochastic.

There are various models that consider user behavior. Some approaches seek to predict the future user consumption based on historical data. The review presented by Swan and Ugursal (2009) contains some of the most common bottom-up approaches to load forecasting. The model presented in Richardson et al. (2010) determines consumption profiles based on the aggregation of individual loads, the number of people in the housing unit, and their activity profiles. In a similar way, Collin et al. (2014) uses a Markov-chain Monte-Carlo model to compute the activity profiles in order to estimate realistic load profiles for a wide variety of housing units. The approach presented in Subbiah et al. (2013) uses logistic and Poisson regression to model the correlational and consistency elements of the shared activities of multiple inhabitants in a household.

The characterization framework in Soares et al. (2014) analyzes the controllable demand and its potential savings for users participating in an energy management system. Similarly, the

approach in Munkhammar et al. (2014) estimates consumption profiles by fitting probability density distributions over a historical set for single and multiple housing units.

The importance of a consumption-aware user is discussed in Nguyen and Aiello (2013). This survey includes elements such as potential energy savings, activities with higher potential impact, and the availability of information and automation in the building.

There are various strategies for integrating the end-users into the grid decisions. In demand-side management approaches, e.g., Fernandes et al. (2014), Chen et al. (2012), and Gomez and Anjos (2017a), the user preferences are typically hard constraints and are met while optimizing the energy consumption or peak reduction. In other cases there is a negotiation process. Multi-objective optimization is used in Korkas et al. (2016) to balance the energy costs and thermal comfort. The user behavior is considered during the process of setting prices in Afsar et al. (2016). In this case a bilevel optimization approach is used to find a trade-off between the revenue obtained by the energy provider and the user dissatisfaction.

Different pricing policies are assessed in Muratori and Rizzoni (2016) and Vardakas et al. (2015) to explore the effect on user participation and grid performance. A pricing policy that considers user behavior facilitates the user's integration into the SG decisions.

In this article we propose a framework to determine day-ahead capacity profiles that account for the stochastic demand generated by the user behavior. This goes beyond a forecasting approach, since it determines how to respond to the expected demand (i.e., the forecast) in an optimal way that minimizes the cost for the users, ensures their satisfaction, and considers the grid requirements. In this framework the user books a level of capacity per time frame in the context of flexible time-and-level-of-use (TLOU) pricing. This pricing policy is an extension of that presented in Gomez and Anjos (2017b).

We generate the consumption scenarios by aggregating the individual historical data for each activity load. We also present two approaches to determine when to book power and how much to book to satisfy the demand. First, we propose a two-stage optimization model that minimizes the cost. Second, we propose a heuristic algorithm that uses a set of previous consumption profiles to estimate future capacity requirements.

The use of capacity profiles gives savings for the users and provides the grid with more information about the operation of the system. One of the main features of this work is that the users do not manage their consumption to follow a fixed cost profile; instead, the utility adjusts the costs to the user preferences while considering the grid requirements.

This article is structured as follows: the proposed approaches are described in Section 5.3, the experimental results and analysis are presented in Section 5.4, and the conclusion is given

in Section 5.5.

5.3 Proposed Framework

Our framework is based on the concept of a capacity profile. A capacity profile allows us to establish a trade-off between user energy requirements and peak-oriented grid decisions. Our framework estimates capacity profiles considering the user behavior and a dynamic cost scheme. The consumer books a maximum level of consumption per time frame, providing the grid with information in advance and receiving energy below that level at a discounted price. The utility uses this information for planning purposes and is able to charge a higher price if the user exceeds the specified level.

A challenge of this type of decision-making is the proper representation of user behavior. The appropriate capacity depends on the demand. We represent the demand as a stochastic parameter derived by aggregating consumption over all the user's activities. Since this information is not always available, we propose a comprehensive framework that supports the decision-making. Figure 5.1 shows the framework representation, finishing with a simulation and cost validation stage.

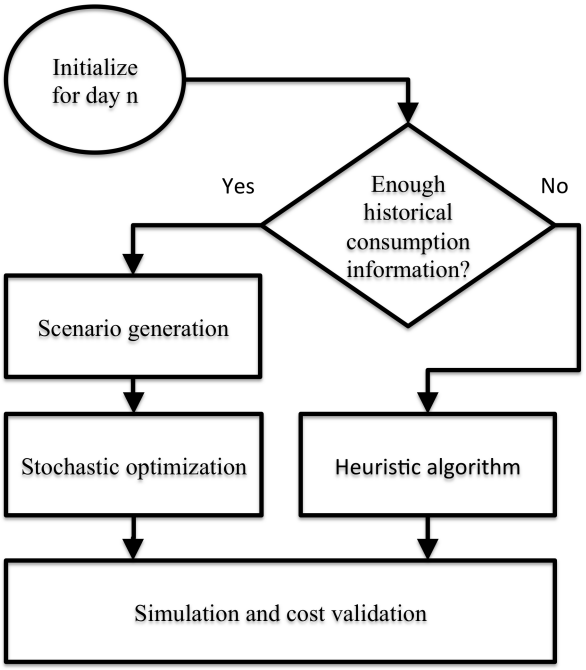

Figure 5.1 Framework to determine capacity profiles for activity-based loads

5.3.1 Flexible TLOU Cost Structure

Time of use (TOU) pricing is widely implemented for the residential sector. Under TOU the price depends on the time of day. Figure 5.2 shows the time windows for off-peak, mid-peak, and on-peak tariffs specified by the Independent Electricity System Operator of Ontario (Canada).

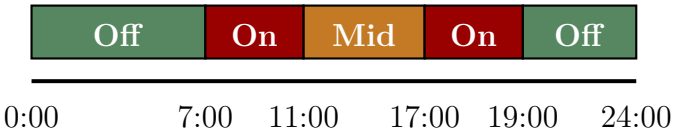

Figure 5.2 Ontario IESO TOU periods in winter.

We use a cost structure that includes another dimension: the price depends on the level of consumption in each time frame. For a specified power limit, consumption up to this limit is charged at a lower tariff, and consumption above this limit is charged at a higher tariff. This time-and-level-of-use pricing was implemented in Gomez and Anjos (2017b), where the tariffs and capacity limits were set by the utility or the grid operator. In the approach presented in this article, the tariff depends on the capacity level booked by the user in each time frame. The utility provides a set of tariffs and capacities from which the consumer can choose. Figure 5.3 shows the possibilities for the lower tariff; this step function has $\mid J \mid$ segments, and the TOU tariff is represented by the parameter K_t^0. Note that all the possible tariffs are $\leq K_t^0$. Selecting $c_t^2 > c_t^1$ allows a cheaper tariff $K_t^{L_2} < K_t^{L_1}$. The higher tariff for consumption above the limit is represented by the function in Figure 5.4. This step function has $\mid Q \mid$ segments, and the possible tariffs are $\geq K_t^0$. In this case booking a lower capacity implies a cheaper tariff.

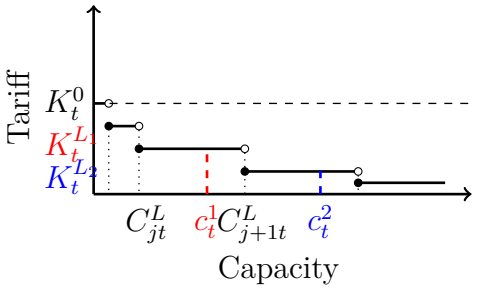

Figure 5.3 Lower energy tariff as a step function of the booked capacity.

Additionally, we introduce a booking fee K_t^F per power unit that is paid in advance by the user. Determining the capacity is thus a nontrivial decision. Booking a higher capacity c_t^2

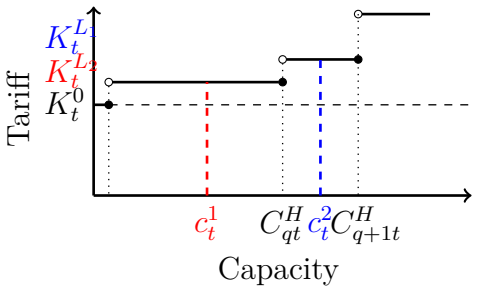

Figure 5.4 Tariff for consumption above limit as a step function of the booked capacity.

will give a cheaper $K_t^{L_2}$ and a more expensive $K_t^{H_2}$ as well as a higher booking cost $K_t^F c^2$.

5.3.2 Scenario Generation

We assume that the start of each load follows a normal distribution. The duration and the level of consumption of each appliance are deterministic parameters.

The aggregation of individual loads can result in numerous scenarios since each time t has $\sum_{m=1}^{|M|} \binom{|M|}{m}$ possible consumption levels obtained from the possible arrivals of the loads. Including zero consumption, we have for each time frame $\sum_{m=1}^{|M|} \binom{|M|}{m} + 1 = \sum_{m=0}^{|M|} \binom{|M|}{m} = 2^{|M|}$ possible consumption levels.

The arrival distribution of each load m is discretized over $\mid T \mid$ time frames, and the probability that load m starts in time frame t is denoted $Pr(X_{mt} = 1)$.

We also need to consider the load durations, so we define the probability that load m is active in time frame t as:

$$Pr(\tilde{X}_{mt} = 1) = \sum_{t-L_m}^{t} Pr(X_{mt} = 1),$$

which is the accumulated probability over the duration of the load. Finally, we compute the probability that scenario i occurs in time frame t as

$$Pr_{it} = \prod_{m \in i} Pr(\tilde{X}_{mt} = 1) \prod_{m \notin i} (1 - Pr(\tilde{X}_{mt} = 1)),$$

where we aggregate the loads m of scenario i. Depending on the parameters of the distribution and the load durations, some of the scenarios can have near-zero probabilities. We remove the scenarios with a probability $< \rho$, where ρ is a significance threshold defined by the decision-maker. The more concentrated the loads are over a set of time frames, the more scenarios can be discarded from this set. Thus, each time frame t can have a different number of scenarios (i.e., $I(t)$).

5.3.3 Two-Stage Stochastic Optimization Model

We estimate the capacity by solving a two-stage optimization problem (Birge and Louveaux, 2011). In the first stage the user determines the capacity required per time frame. The second stage takes into account the cost of meeting the demand and the costs associated with the decision. The objective function (5.1) includes the booking cost, the expected cost of consumption at the lower tariff, and the expected cost of consumption at the higher tariff.

$$\min \sum_{t\in T}\sum_{j\in J} K_t^F c_{jt} + \sum_{t\in T}\sum_{j\in J}\sum_{i\in I(t)} Pr_{it} K_{jt}^L x_{ijt}^L + \sum_{t\in T}\sum_{q\in Q}\sum_{i\in I(t)} Pr_{it} K_{qt}^H x_{iqt}^H \tag{5.1}$$

subject to

$$\sum_{j\in J} \phi_{jt} = 1 \quad \forall t \in T \tag{5.2}$$

$$\sum_{q\in Q} \delta_{qt} = 1 \quad \forall t \in T \tag{5.3}$$

$$\phi_{jt} C_{jt}^L \leq c_{jt} \leq \phi_{jt} C_{j+1t}^L \quad \forall j \in J \mid j <\mid J \mid -1, t \in T \tag{5.4}$$

$$\delta_{qt} C_{qt}^H \leq \bar{c}_{qt} \leq \delta_{qt} C_{q+1t}^H \quad \forall q \in Q \mid q <\mid Q \mid -1, t \in T \tag{5.5}$$

$$\sum_{j\in J} c_{jt} - \sum_{q\in Q} \bar{c}_{qt} = 0 \quad \forall t \in T \tag{5.6}$$

$$x_{ijt}^L \leq c_{jt} \quad \forall i \in I(t), j \in J, t \in T \tag{5.7}$$

$$\sum_{j\in J} x_{ijt}^L + \sum_{q\in Q} x_{iqt}^H \geq D_{it} \quad \forall i \in I(t), t \in T \tag{5.8}$$

$$x_{ijt}^L, x_{iqt}^H, c_{jt}, \bar{c}_{qt} \geq 0, \quad \forall i \in I(t), j \in J, q \in Q, t \in T \tag{5.9}$$

$$\phi_{jt}, \delta_{qt} \in \{0, 1\} \quad \forall j \in J, q \in Q, t \in T \tag{5.10}$$

Constraints (5.2) and (5.3) ensure that the booked capacity belongs to one of the intervals of the step functions for both tariffs. Constraints (5.4) and (5.5) set the lower and upper bounds for each interval of the step functions. We introduce the auxiliary variable $\bar{c}_{qt}$ for the capacity in the higher-tariff step cost function. Constraint (5.6) establishes the relationship between the capacity and the auxiliary variable.
Constraints (5.7) and (5.8) impose the lower-tariff consumption and the demand satisfaction, respectively, for each scenario. Finally, constraints (5.9) and (5.10) are the nonnegativity and binary constraints.

In the model the capacity requirements are computed by time frame; in a more realistic scenario the grid operator could assign capacity profiles over a longer horizon of consumption.

In the context of TOU we can identify several time windows (groups of time frames) with the same price (for example, off-peak, mid-peak, and on-peak tariffs). Given a set Ω of time windows, we could enforce the same capacity for the time frames in the same time window by adding constraint (5.11):

$$c_{jt} = c_{jt'} \quad \forall j \in J, \quad t, t' \in \tau^{\omega} \mid t \neq t', \quad \omega \in \Omega \tag{5.11}$$

where $\tau^{\omega} \subset T$ is a subset of time frames. This modification to the original model will be explored in Section 5.4.

5.3.4 Heuristic Approach

Figure 5.5 shows two possible realizations of the capacity (dashed red line) required to operate two loads in some time frame. Booking the complete area will be costly if the total booking cost is greater than the savings associated with the cheaper tariff.

The approach presented in this section reduces the area under the dashed red line by using information about which time frames are more likely to receive loads. This consumption information is contained in the matrix $\Gamma \in \mathbb{R}^{N \times |T|}$ for a set of N previous days. We use the data in Γ to split the horizon into several segments S and then to allocate a capacity c_t to each time frame.

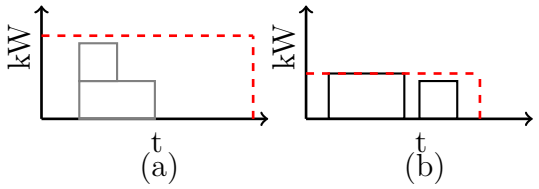

Figure 5.5 Capacity profile area reduction.

First, we identify several contiguous submatrices in Γ by clustering time frames based on proximity and consumption. Each submatrix contains either only time frames with no consumption (columns of zeros) or columns with some consumption over the historical set. Equation (5.12) shows Γ for three days and six time frames; we can identify four segments: columns 1, 2–3, 4–5, and 6.

$$\Gamma = \begin{pmatrix} \mathbf{0} & 0 & \lambda & \mathbf{0} & \mathbf{0} & 0 \\ \mathbf{0} & \epsilon & 0 & \mathbf{0} & \mathbf{0} & \lambda \\ \mathbf{0} & 0 & \eta & \mathbf{0} & \mathbf{0} & 0 \end{pmatrix} \tag{5.12}$$

After this identification we discard the time frames where loads are not expected based on

the historical data.

Second, we compute the capacity profile by assigning the average consumption for each time frame. We must decide the size of N before determining the capacity profile. Too few days (rows) in Γ could result in insufficient information. On the other hand, increasing the number of days may not add significant information or could introduce rare events that do not represent typical user behavior. Experimentally we observe that as the number of days increases, the number of segments stabilizes because of the finite horizon. We continue including days and identifying segments until we have added β days without changing the number of segments. Algorithm 1 presents this process in detail.

Algorithm 1 Capacity profile for activity-based loads

Initialization

- $n = 0$ Iteration number (i.e., days added)
- $\alpha = 0$ Number of iterations with the same number of segments

Obtain number of segments

while $\alpha < \beta$ **do**
  $n \leftarrow n + 1$
Add a row to Γ
Compute $\bar{S}(n)$ by identifying the number of intervals in Γ
  if $\bar{S}(n) = \bar{S}(n-1)$ **then**
    $\alpha = \alpha + 1$
  else
    $\alpha = 0$
  end if
end while
$N \leftarrow n$
$S \leftarrow \bar{S}(n)$

Compute profile

$c_t \leftarrow (\sum_{n=1}^{N} \Gamma_{n,t})/N \quad \forall \quad t \in T$

Algorithm termination

We prove that Algorithm 1 terminates by proving the existence of an upper bound for $\bar{S}(n)$ and monotonically decreasing behavior after this maximum value has been reached.

Let z_t^n be a parameter indicating whether or not column t of matrix Γ at iteration n is an

all-zero column:

$$z_t^n = \begin{cases} 1 & \text{If column } t \text{ is zero} \\ 0 & \text{Otherwise} \end{cases}$$

We can determine the number of segments via:

$$\bar{S}(n) = y(n) + 1$$

where $y(n)$ is the number of transitions between zero and nonzero columns, and $\bar{S}(n)$ is an integer value in the interval $[0, \mid T \mid]$:

$$y(n) = \sum_{t=1}^{|T|-1} (z_t^n - z_{t+1}^n)^2.$$

Lemma 1. *There exists $S^{\max}$ such that $\bar{S}(n) \leq S^{\max}$ for a given horizon $\mid T \mid$.*

Proof. The maximum value for each pair $(z_t^n - z_{t+1}^n)^2 = 1$, so $y^{\max} \leq \mid T \mid -1$ and $S^{\max} \leq \mid T \mid$. Therefore, $S^{\max}$ exists. □

Lemma 2. *After $\bar{S}(n)$ reaches $S^{\max}$, $\bar{S}(n)$ is monotonically decreasing.*

Proof. We know that the number of rows in Γ increases at each iteration, so

$$z_t^{n+1} \geq z_t^n, \quad \forall \quad n = 1 \ldots N, \quad \forall \quad t \in T.$$

If $z_t^{n+1} = z_t^n \quad \forall \quad t \in T$, then $y(n+1) = y(n)$ and $\bar{S}(n+1) = \bar{S}(n)$.

If there exists t such that $z_t^{n+1} > z_t^n$, then there exists a pair $(z_t^n - z_{t+1}^n)^2 = 0$, $y(n+1) \leq y(n) - 1$, and $\bar{S}(n+1) \leq \bar{S}(n) - 1$. □

Theorem 1. *Algorithm 1 terminates.*

Proof. Because $y \geq 0$ and $S \geq 0$, by lemma 2 the algorithm must terminate. □

5.4 Experimental Results

5.4.1 Stochastic Optimization

We explore changing the number of loads, the standard deviation of the arrivals, and the concentration of the average arrival time (i.e., how close the arrivals are to each other). The

first impacts the number of scenarios and the aggregated consumption level; the second and third affect the congestion over a time window. We denote the instances with $\Phi_{|M|\sigma\bar{x}}$ where $\mid M \mid = \{3, 5, 10\}$, $\sigma = \{0.5, 2, 4\}$, and $\bar{x} = \{1$: low, 2: medium, 3: high$\}$ concentrations of the arrival of the loads over similar time frames. Figure 5.6 shows the values for $\bar{x}$.

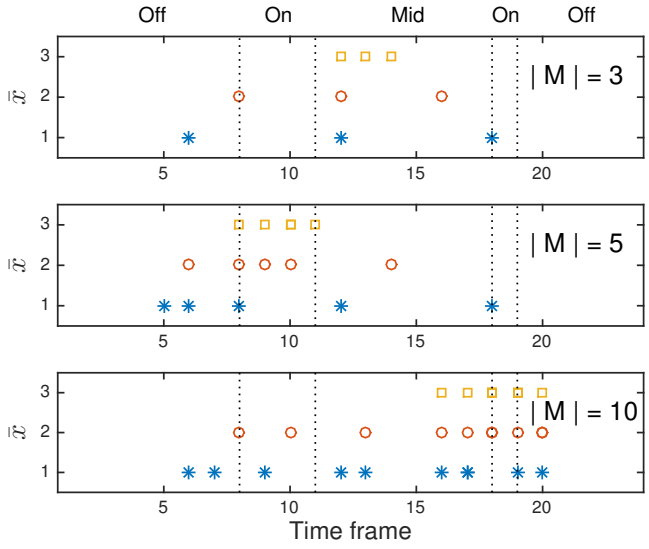

Figure 5.6 Concentration of load arrivals.

We observe that the activities become closer as $\bar{x}$ increases. They cluster in the mid-peak frames for $\mid M \mid = 3$, in the on-peak frames for $\mid M \mid = 5$, and spread over the evening for $\mid M \mid = 10$.

Figure 5.7 shows the resulting expected consumption profiles. These are computed with the information from Figure 5.6, combined with each value in σ and taking into account the duration of the loads. The consumption peaks are typically generated when the concentration $\bar{x}$ is high and σ is low. In these cases the higher tariff of the TLOU accounts for the additional costs that the grid incurs to maintain the balance between supply and demand.

Table 5.1 shows the total cost and accumulated capacity c^{tot} over the horizon, obtained by solving the problem for all combinations of the parameters previously introduced as well as both versions of the model presented in Section 5.3.3: Model 1: equations (5.1)–(5.10) and Model 2: equations (5.1)–(5.11).

We observe that none of the parameters or models has clear behavior with respect to the total capacity. A higher $\mid M \mid$ (i.e., higher total demand) does not always lead to the booking of more capacity. This counterintuitive behavior is repeated for σ, $\bar{x}$, and both versions of the model. At this point we need to consider the interaction of the parameters to understand

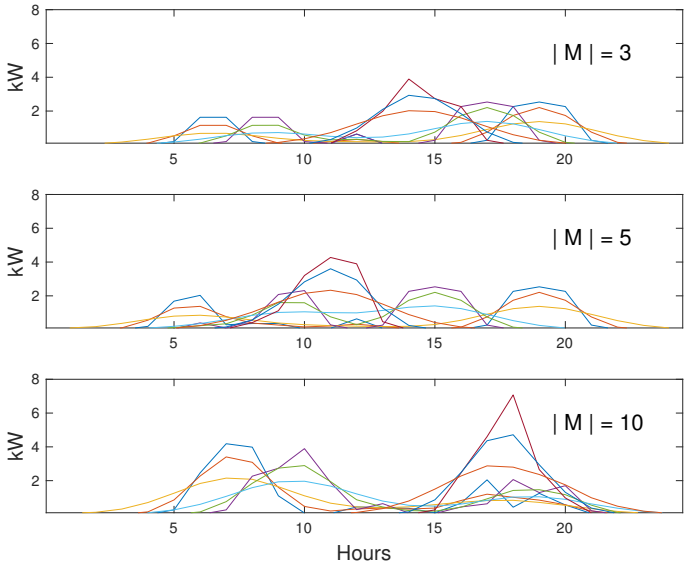

Figure 5.7 Expected consumption profiles.

how the optimization is working, since they determine the shape of the expected demand curve. Figures 5.8 and 5.9 give examples.

We change σ in Figures 5.8(a) and 5.8(b) while keeping the other parameters constant. For $\sigma = 0.5$ we obtain $c^{tot} = 13.3$. A higher $\sigma = 1.0$ flattens the expected demand curve, resulting in a lower $c^{tot} = 12.2$. Similarly, we change σ in Figures 5.8(c) and 5.8(d), this time with $\bar{x} = 3$. In this case we end up with a higher c^{max} for $\sigma = 1.0$. Although the demand curve is flattened, it is still high enough to make it economical to buy capacity in advance, due to the proximity of the different loads over time. We can see this clearly at $t = 13$, where the expected demand changes from 0.1 in 5.8(c) to 1.1 in 5.8(d).

The selection of the negotiation frequency is represented in model 1 (each time frame) and model 2 (each time window). Figure 5.9 shows an example of this.

Figures 5.9(a) and 5.9(b) show the results of the model variations for the same instance. The hourly negotiation in 5.9(a) gives a higher c^{tot} than does the window negotiation from 5.9(b). The dispersed expected demand makes it inefficient to buy capacity for a full time window.

We observe opposite behavior in Figures 5.9(c) and 5.9(d). In this case, the way the expected demand curve fits the defined time windows will give a higher c^{tot} by negotiating at every time window.

Note that we are analyzing the conditions where the user chooses to buy more or less capacity, and we are not comparing the costs directly since the models are different. In every case,

Table 5.1 Total cost (¢) and total capacity (kWh) for the instances

	$\mid M \mid = 3$				$\mid M \mid = 5$				$\mid M \mid = 10$			
Instance	Model 1		Model 2		Model 1		Model 2		Model 1		Model 2	
	Cost	c^{tot}	Cost	c^{tot}	Cost	c^{tot}	Cost	c^{tot}	Cost	c^{tot}	Cost	c^{tot}
$\Phi_{\mid M \mid 0.5,1}$	142.7	12.3	147.5	5.0	158.6	13.6	164.3	5.0	217.8	23.8	242.3	3.0
$\Phi_{\mid M \mid 1.0,1}$	147.0	11.5	149.0	5.0	159.4	11.5	161.7	5.0	226.3	21.5	240.5	3.0
$\Phi_{\mid M \mid 2.0,1}$	149.6	7.5	149.8	5.0	161.6	7.5	161.8	5.0	232.5	16.0	236.8	8.0
$\Phi_{\mid M \mid 0.5,2}$	171.2	12.3	186.5	5.0	181.6	13.3	193.9	23.0	271.8	22.7	276.6	20.0
$\Phi_{\mid M \mid 1.0,2}$	172.1	11.5	179.8	5.0	184.9	12.2	190.2	23.0	267.5	21.3	268.6	20.0
$\Phi_{\mid M \mid 2.0,2}$	169.0	7.5	170.5	0.0	188.2	10.5	189.4	14.0	255.2	16.5	256.1	11.0
$\Phi_{\mid M \mid 0.5,3}$	141.8	15.3	149.7	24.0	190.0	19.4	207.6	16.0	237.3	23.0	254.7	14.2
$\Phi_{\mid M \mid 1.0,3}$	147.4	14.8	151.6	24.0	193.3	20.8	204.0	16.0	223.7	24.0	236.9	12.0
$\Phi_{\mid M \mid 2.0,3}$	161.7	14.5	162.7	12.0	194.8	16.5	199.4	16.0	212.2	24.5	220.2	12.0

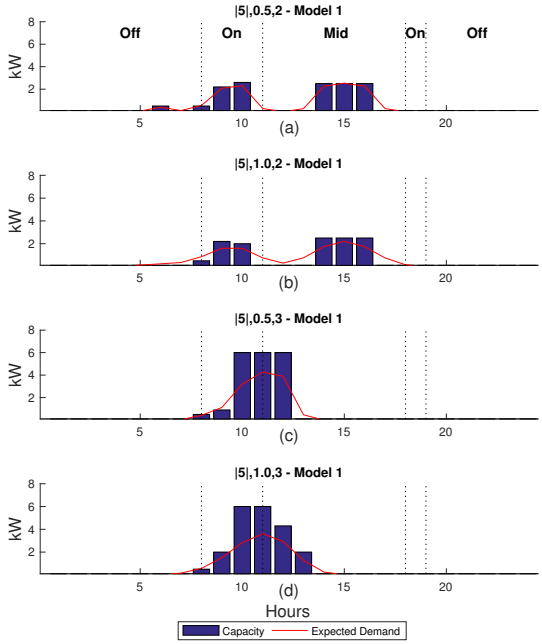

Figure 5.8 Example of effect of σ and $\bar{x}$ on c^{tot}.

hourly booking is cheaper than booking for a complete window. The latter can be interpreted as a trade-off between simplicity for the utility and savings for the user.

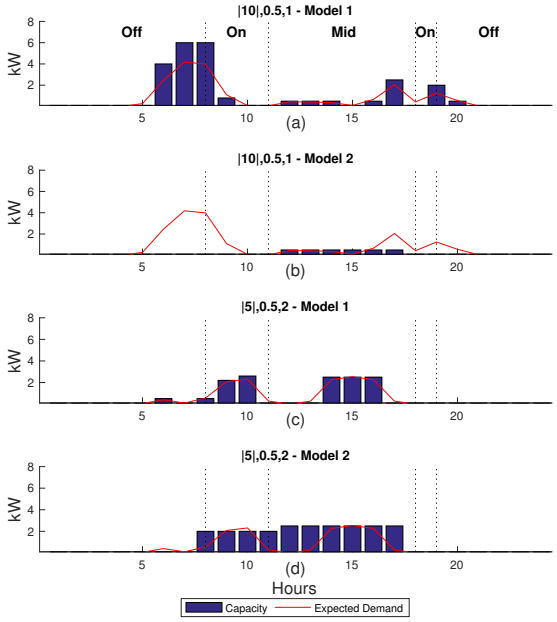

Figure 5.9 Example of the effect of negotiation frequency.

Necessary condition for booking capacity

In Figures 5.8 and 5.9 we see that some time frames with an expected demand greater than zero do not have any capacity booked, even in an hourly negotiation policy.

We can compare the objective function (5.1) for a single time frame where it was better not to book instead of booking c (for simplicity we do not include the cost intervals from the step functions):

$$K^F 0 + \sum_{i \in I} Pr_i D_i K^0 < K^F c + \sum_{i \in I} Pr_i [x_i^L K^L(c) + x_i^H K^H(c)] \tag{5.13}$$

Because $D_i = x_i^L + x_i^H$, we can reorganize equation (5.13) as

$$\sum_{i \in I} Pr_i [x_i^L [K^0 - K^L(c)] + x_i^H [K^0 - K^H(c)]] < K^F c, \tag{5.14}$$

where we find a clear relationship: *the net expected savings must be less than the fixed cost from booking capacity* c. The net expected savings are the savings from the lower tariff and the extra cost of consumption at the higher tariff. The optimization seeks a c that violates the condition in equation (5.14). If such a c does not exist, it is optimal to retain the TOU pricing K^0.

Because equation (5.14) depends strongly on the tariffs, and the tariffs vary depending on the TOU, we observe different behavior for different time frames. We can see this situation in Figure 5.8(b), where the user buys capacity at $t = 8$, an on-peak period, and not at $t = 13$, a mid-peak period, despite the similar expected demands.

5.4.2 Simulation

In this section we implement a 180-day simulation corresponding to the period of the TOU winter tariff in Ontario. We generate each day's consumption randomly given the normal distributions from all the instances introduced in Section 5.4.1. We compare the total cost of the complete simulation for four different approaches: no booking of capacity, booking capacity based on the heuristic approach, and booking it based on our two optimization models.

In the first case, the user pays the TOU tariff originally offered by the utility. In the second case, the user determines the capacity profile with the heuristic value and accepts the K_t^L and K_t^H corresponding to the capacity value. Note that the heuristic does not take into account the cost. Finally, the two models determine both the capacity and the tariffs at the beginning of the simulation as optimal policies.

Figure 5.10 compares the costs of the 27 instances. The optimal hourly negotiation has the best performance for all the instances. As mentioned previously, time-window negotiation represents a trade-off between grid management and potential user savings, giving optimal values that are between the optimal hourly negotiation values and those of the no-booking policy for all the instances. Finally, in both models the average costs are similar to those in Table 5.1. In general terms the user achieves savings of up to 16% by using model 1 rather than TOU only.

The heuristic approach works well in some cases, occasionally reaching values similar to those of model 2. The heuristic is useful in situations where insufficient information is available: it provides suboptimal solutions until the optimization model is ready (i.e., the distributions are known). It could also be helpful for transitions where the user behavior changes and the previous optimal solution is no longer appropriate.

We also observe that the heuristic has poor performance for some instances. These instances have the property that the optimal values for both models are close to the no-booking policy. In these cases, the optimization models either return a low capacity or the savings are not significant because of the shape of the expected demand curve, and the heuristic is not able to determine if booking is a good policy.

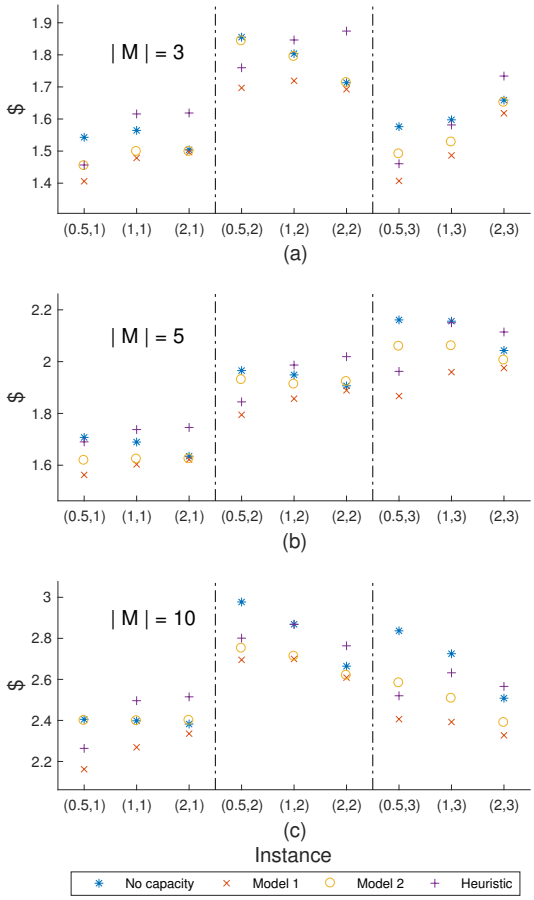

Figure 5.10 Average cost per day for the instances $(\sigma, \bar{x})$.

In general, the approaches perform better when it makes sense to buy capacity in advance. They could be used in combination with demand-side management to support a learning process (optimal consumption) and eventually give more benefits to the user.

5.5 Conclusion

We have proposed a new framework that allows end-users to profit from a novel flexible TLOU tariff in a DR context.

The framework starts with the generation of consumption scenarios by aggregating historical data. We have presented two approaches to help the user determine the required capacity given the demand. The first approach solves a two-stage optimization model under the assumption that the start time probability distributions of the loads are known. The second approach uses a greedy-type algorithm that analyzes a set of previous consumption profiles

to estimate future capacity requirements.

The use of capacity profiles contributes to the expansion of DR in the residential and commercial sectors, allowing consumers to take advantage of lower prices and providing utilities with a tool that helps to compensate for the extra cost of matching generation and demand in congestion periods.

We have provided several scenarios and instances to validate the ideas underlying our approaches. An important aspect of this work is that we consider the user perspective, ensuring satisfaction and obtaining benefits in all the instances. The user does not change his/her preferences and always satisfies his/her energy requirements. The experimental results provide insight into how consumers can modify their expected demand curves to gain greater benefits.

Acknowledgments

This research was supported by the Canada Research Chair on Discrete Nonlinear Optimization in Engineering and by the NSERC Energy Storage Technology Network.

CHAPTER 6 ARTICLE 3: COLLABORATIVE DEMAND-RESPONSE PLANNER FOR SMART BUILDINGS

Authors: Juan A. Gomez, Miguel F. Anjos.
Submitted to: Energy and Buildings

Abstract

This work presents a collaborative scheme for the end-users in a smart building with multiple housing units. This approach determines a day-ahead operational plan that provides demand-response services by taking into account the amount of energy consumed per household, the use of storage and solar panels, and the amount of shifted load. We use a biobjective optimization model to trade off total user satisfaction versus total cost of energy consumption. The optimization works in combination with a novel cost structure based on time and level of use that encourages load shifting and benefits the participants. Experimental results and a sensitivity analysis validate the performance of the proposed approach and help to clarify its strengths, its limits, and the requirements for ensuring the desired outcome.

Keywords

Smart Buildings, Demand-Response, Residential Load, Biobjective Optimization, Compromise Programming.

6.1 Notation

Sets:

$i \in I$: Energy levels
$j \in J$: Users
$t \in T$: Time frames

Parameters:

D_{jt} : Energy demand of user j in time frame t

K_{it} : Cost per energy unit bought from the grid in level i in time frame t

C^L : Available capacity in the lower level

C_j^H : Available capacity in the higher level for user j

B : Cost of charging the battery per energy unit

S^{max} : Capacity of the battery

Γ : Battery efficiency

Z : Number of cycles allowed in the battery

P_t : Incentive paid by the grid per energy unit in a demand-response call in time frame t

DR_t : Energy consumption reduction requested by the grid in time frame t

G_t^{max} : Available energy from solar panels in time frame t

F : Cost per energy unit obtained from the solar panels

Y_j : Total backlogged demand over the horizon accepted by user j

$\hat{Y}_j$: Max backlogged demand at the end of the horizon for user j

Ψ_{sol}^{max} : Max percentage of total demand satisfied by solar panels

Ψ_{sol}^{min} : Min percentage of total demand satisfied by solar panels

Ψ_{bat}^{max} : Max percentage of total demand satisfied by the battery

Ψ_{bat}^{min} : Min percentage of total demand satisfied by the battery

Variables:

x_{ijt} : Energy bought from the grid in level i by user j in time frame t

y_{jt} : Accumulated unmet demand at the end of period t for user j

soc_{jt} : Individual state of charge for user j at the end of time frame t

s_{jt}^+ : Energy charged in the battery in time frame t by user j

s_{jt}^- : Energy discharged from the battery in time frame t by user j

r_{jt} : Amount of demand-response service provided by user j in time frame t

g_{jt} : Consumed energy from solar panels for user j in time frame t

α_t :
$$\begin{cases} 1 & \text{Battery charges during time frame } t \\ 0 & \text{Battery discharges during time frame } t \end{cases}$$

z_t :
$$\begin{cases} 1 & \text{Battery changes from charging to discharging or vice versa} \\ 0 & \text{Otherwise} \end{cases}$$

ϕ_t :
$$\begin{cases} 1 & \text{The building agrees to provide demand response in time frame } t \\ 0 & \text{Otherwise} \end{cases}$$

6.2 Introduction

The implementation of smart buildings introduces two major challenges for consumer planning. First, consumers desire to meet their energy requirements keeping a high level of satisfaction at a minimum cost. These objectives can rarely be attained simultaneously. Second, the energy supplier (system operator, utility, etc.) is required to meet user demand while ensuring system stability. It is often difficult to satisfy these requirements during peak consumption times.

The end-users play an important role in the mission of balancing generation and demand. This participation is driven mainly by a) demand response (DR), defined as changes in consumers' usage in response to incentives designed by the energy supplier to induce lower consumption (FERC, 2012), and b) smart grids, which support communication and decision-making by both users and generators. These technologies also allow the integration of new resources, such as distributed generators, solar panels, and storage units, that increase the complexity of the system but may offer benefits to all the participants.

The residential and commercial sectors represent a major part of the total consumer demand (EIA, 2016). The aggregated DR potential in these sectors could be important in the current and future operation of the grid, but it is difficult to exploit due to the large number of users. An entity capable of coordinating the DR programs of this group of consumers could profit from economies of scale. The approach presented in this article aims to support and facilitate this coordination process.

Previous work referred to this aggregated system in the presence of storage and/or distributed generation as a microgrid. The comprehensive review presented in Parhizi et al. (2015) introduces various aspects of microgrids, including operation, investment, generation technologies, communications requirements, and grid-support and islanding capabilities.

Some works focus specifically on the planning and control of the system. The approach in Parisio et al. (2014) controls the operation of a microgrid in a realistic scenario. It schedules generators, storage devices, and controllable loads, and it compensates for the uncertainties in the dynamics of the system through a model predictive control strategy.

A similar idea is explored in Kriett and Salani (2012), including models for combined heat and power generation, in the presence of thermal and electrical loads and storage units. An economic comparison of a rolling-horizon approach and the standard unit commitment for microgrids is presented in Palma-Behnke et al. (2013).

The algorithm presented in Mhanna et al. (2016) schedules loads for large populations. It aggregates different types of appliances and distributed energy systems.

Some other studies consider the integration of the microgrids into the distribution system. The mixed integer programs in Mesari and Krajcar (2015) and AlSkaif et al. (2017) minimize the use of conventional generation resources in order to encourage the use of the batteries of electric vehicles and the available renewable resources, ensuring a high level of self-consumption. The approach presented in Chabaud et al. (2015) assesses several configurations of a grid-connected microgrid, considering a two-way flow of power and its impact on the grid. An autonomous microgrid optimal operation approach is presented in Detroja (2016), considering the generation and consumption sides and the balance between the two in a real-time scenario. A function based on declining block rates achieves a balance between user comfort and electricity cost in Hasib et al. (2015). It presents a microeconomic analysis of this function, and the method is used for bidirectional energy trading.

All the approaches mentioned previously minimize the total operational cost. Some of them take into account elements such as user comfort and preferences via constraints and/or costs that approximate the level of satisfaction. This way of dealing with conflicting objectives is one among several options in multiobjective optimization (Ehrgott, 2006). When objectives conflict, such as cost and comfort in our case, there is usually no solution that optimizes them simultaneously. To improve one of the objectives we may have to worsen one or more of the others. When this is the case, the solution is said to be Pareto efficient, Pareto optimal, or nondominated.

A comprehensive review of methods to find Pareto efficient solutions can be found in Marler and Arora (2004). It presents approaches that include the user preferences in the decision-making and that represent and approximate the Pareto front (the set of Pareto efficient solutions).

Multiobjective optimization has been explored in the smart grid context. Particle swarm optimization and weighted aggregation are used in Yang and Wang (2012) to approximate the Pareto front for energy cost and environment comfort. The Pareto front is approximated using the ϵ-constraint method in Zhang et al. (2012), balancing the total cost and the energy obtained from distributed generators in isolated sites, and in Hosseinnezhad et al. (2016) and Aghaei and Alizadeh (2013) minimizing both pollutant emission and operating cost.

The weighted-sum approach is used to balance the minimization of load curtailment, operating cost, and pollutant emission in Cao et al. (2017), and energy costs and thermal comfort in Korkas et al. (2016).

Finally, lexicographic goal programming is used in Choobineh and Mohagheghi (2016) to minimize the operational costs, the emissions produced, and the asset deterioration resulting from exposure to excess temperatures.

This paper proposes a novel framework to determine an operational plan for a smart building with multiple housing units. The framework considers grid requirements and balances cost and satisfaction for the end-users. We use biobjective optimization to find efficient trade-offs between the two conflicting objectives without estimating the Pareto front. This is combined with production planning concepts and models to achieve a realistic representation for the smart grid context. In this scenario the consumers may actively participate, choosing when to shift load. In combination with a shared storage unit and a set of solar panels available in the smart building, this option allows the participants to profit from the pricing policies and incentives while providing DR.
This paper is structured as follows. The proposed approach is described in Section 6.3, the experimental results and sensitivity analysis are presented in Section 6.4, and the conclusion is given in Section 6.5.

6.3 Proposed Optimization Approach

Figure 6.1 shows the general operation of the smart building. The planning module receives day-ahead information from all the households and resources: user preferences, forecasts of energy demand and solar radiation, battery state of charge, and scheduled DR requests from the grid. It is important to highlight that the battery and a set of solar panels are managed by the building, and they are resources that are shared among all the housing units. Once all the information has been gathered, the planner solves a biobjective optimization problem for the building, finding a trade-off between the total cost and the shifted load. The shifted load represents the level of dissatisfaction perceived by the user; each user submits preferences indicating when and by how much he/she is prepared to delay or reduce consumption.

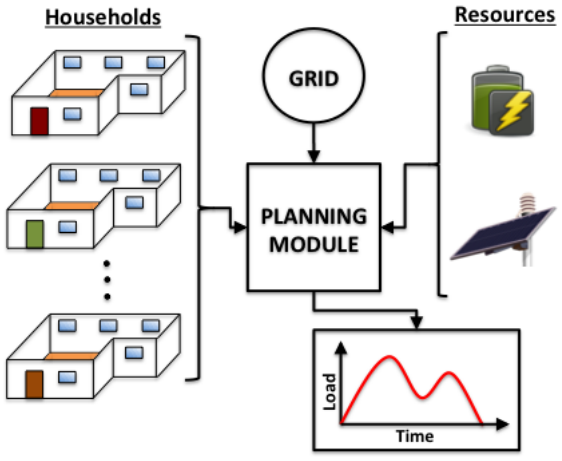

Figure 6.1 Smart building operation.

After solving the optimization problem, we obtain individual plans that specify for each time frame t the amount of energy to be drawn from the grid, the allocation of the energy obtained from the solar panels, the use of the battery, and the shifted load for each user j.

One of the main features of this approach is that it finds a balance between the two objectives while providing DR services. We include two of the most common types of DR: incentive-based programs and pricing programs (Siano, 2014). For the incentive-based program the optimization model decides whether or not the building answers a DR call. In the case of a positive answer, the building commits to lowering consumption by using the battery or allocating capacity reductions to some customers, who shift load accordingly. Finally, it reports to each household its share of the DR provided and the benefit obtained. The pricing program encourages peak reduction through the combination of different prices.

We propose a *time and level of use (TLOU) pricing structure* in which the price varies time-wise and level-wise. This is an extension of the time of use (TOU) pricing that is widely used. The TLOU pricing is represented by the parameter K_{it}. In each time frame t, each user can consume up to capacity i, paying price K_{it}. Beyond this threshold the user will pay the next price, $K_{i+1,t}$. We consider two pricing levels for each time frame, a *lower* price and a *higher* price, but in general several levels can be used. This pricing structure works in combination with the DR requests from the grid and the willingness to shift load. Its effect is strengthened via the use of the storage unit and solar panels. The costs associated with these two resources represent the amortization of the corresponding investments.

6.3.1 Similarity to the Lot-Sizing Problem

In a general way, determining the consumption plan under these conditions resembles a classical manufacturing problem: the lot sizing (LS) problem. LS determines the lot sizes that minimize the operational cost of a production process over a multiperiod horizon (Pochet and Wolsey, 2006). We must determine the amount of energy to consume in each time frame. Each user has maximum consumptions C^L and C_j^H and is willing to shift load according to the preference parameters Y_j and $\hat{Y}_j$. This is similar to capacitated LS with backlogging (Pochet and Wolsey, 2006), where the objective is to minimize the sum of the production, storage, and backlogging costs. We assess the cost of shifting load (backlogging) by solving a biobjective optimization problem via compromise programming.

6.3.2 Compromise Programming

As mentioned in Section 6.2, there are different ways to solve a multiobjective optimization problem. All of them seek a trade-off between the conflicting objectives. This is normally represented in the criterion space, which is an image of the feasible set of the optimization problem in terms of the objective functions. Figure 6.2 shows the Pareto front (dashed red line), the feasible region (gray area), and the two objectives to be minimized (f_1 and f_2).

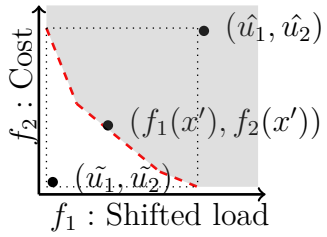

Figure 6.2 Generic description of criterion space.

The ideal or utopia point $(\tilde{u_1}, \tilde{u_2})$ is a point where all the objectives achieve their individual optima. Since the objectives conflict, the utopia point is infeasible. Therefore, we want to find a point on the Pareto front that is a fair approximation of the utopia point. Compromise programming finds a Pareto-efficient solution x' that minimizes the Euclidean distance with respect to the utopia point (Marler and Arora, 2004). We use compromise programming since we can directly obtain an efficient solution that represents the policy adopted by the building. The optimization model can easily be adapted to other approaches such as e-constraint and normal boundary intersection, if a representation of the Pareto front is required; for example, if the policy changes over time.

We are dealing with objectives with different units and different orders of magnitude, so it is necessary to normalize their values. We use the nadir point $(\hat{u}_1, \hat{u}_2)$ and the utopia point for the normalization, since they provide tight upper and lower bounds (dotted lines) on the nondominated solution set.

We follow these steps to find the compromise solution. First, we solve the optimization problem for each of the individual objectives to compute $\tilde{u_1}$ and $\tilde{u_2}$. We then use the optimal solutions to compute $\hat{u}_1$ and $\hat{u}_2$. Finally we solve a mixed binary quadratic optimization problem to find the closest feasible point to the utopia point. This approach allows us to find a trade-off between the two objectives without approximating the complete Pareto front. Moreover, the objective function remains convex, so the full problem can be solved efficiently by off-the-shelf solvers.

6.3.3 Optimization Model

The objective function in equation (6.1) minimizes the squared distance to the utopia point. Equations (6.2) and (6.3) account for the shifted load and the total cost respectively. Equation (6.3) includes the cost of the energy bought from the grid, the cost of using the battery and solar panels, and the incentive paid to the end-users for the DR requests.

$$\min_{f} \quad \left(\frac{f_1 - \tilde{u_1}}{\hat{u}_1 - \tilde{u_1}}\right)^2 + \left(\frac{f_2 - \tilde{u_2}}{\hat{u}_2 - \tilde{u_2}}\right)^2 \tag{6.1}$$

$$f_1 = \sum_{j \in J} \sum_{t \in T} y_{jt} \tag{6.2}$$

$$\begin{aligned} f_2 = &\sum_{i \in I} \sum_{j \in J} \sum_{t \in T} K_{it} x_{ijt} + \sum_{j \in J} \sum_{t \in T} B s^+_{jt} \\ &+ \sum_{j \in J} \sum_{t \in T} F g_{jt} - \sum_{j \in J} \sum_{t \in T} L_t r_{jt} \end{aligned} \tag{6.3}$$

Next, we introduce the constraints. Constraints (6.4) and (6.5) account for the shifting preferences. In (6.4) we enforce the maximum accumulated shifted load for each user j throughout the time horizon. Through (6.5) each user is able to specify the maximum acceptable unmet demand at the end of the horizon. In other words, a user can be flexible about when the demand is satisfied but strict about having it met by the end of the day.

$$\sum_{t \in T} y_{jt} \leq Y_j \qquad \forall \;\; j \in J \tag{6.4}$$

$$y_{jn} \leq \hat{Y}_j \qquad \forall \;\; j \in J \tag{6.5}$$

The maximum amount of energy that can be drawn from the grid is shown in constraints (6.6) and (6.7).

$$x_{1jt} \leq C^L \qquad \forall \;\; j \in J, \;\; \forall \;\; t \in T \tag{6.6}$$

$$x_{2jt} \leq C^H_j \qquad \forall \;\; j \in J, \;\; \forall \;\; t \in T \tag{6.7}$$

The parameter C^L is defined by the grid and is given to all the users to ensure a minimal operation. On the other hand, C^H_j depends on each user and represents a large constant from the optimization point of view; we will revisit this definition in Section 6.4.1.

Constraints (6.8) and (6.9) limit the capacity of the solar panels and the battery respectively (battery expressed as a percentage of S^{max}).

$$\sum_{j \in J} g_{jt} \leq G_t^{max} \qquad \forall \ \ t \in T \tag{6.8}$$

$$\sum_{j \in J} soc_{jt} \leq 1 \qquad \forall \ \ t \in T \tag{6.9}$$

The flow conservation is represented in a similar way to that of LS. Constraint (6.10) ensures that the inflows and outflows are balanced at every time step. It differs from LS in that it accounts for the efficiency Γ of the battery, which depends on the actual flow of energy and not on the state of charge.

$$\begin{aligned} &\sum_{i \in I} x_{ijt} + g_{jt} + y_{jt} + \Gamma s_{jt}^{-} \\ &= y_{jt-1} + D_{jt} + s_{jt}^{+} \quad \forall \ \ j \in J, \ \ \forall \ \ t \in T \end{aligned} \tag{6.10}$$

A common feature of LS is the presence of Wagner–Whitin costs. This cost structure favors production at the time of the demand. The use of storage or the backlogging of orders is penalized; this is traditionally the ideal scenario in manufacturing processes. Wagner–Whitin costs normally simplify the modeling stages in LS because they discard solutions that are suboptimal and do not make sense in a realistic scenario. We use TLOU pricing rather than Wagner–Whitin costs; an analysis of our cost scheme is presented in Section 6.4. Moreover, we penalize backlogging through the biobjective approach without a specific monetary cost. We include constraint (6.11) to avoid charging the battery with backlogged load; it describes the physical energy flow toward the battery.

$$g_{jt} + \sum_{i \in I} x_{ijt} - s_{jt}^{+} \geq 0 \qquad \forall \ \ j \in J, \ \forall \ \ t \in T \tag{6.11}$$

Constraints (6.12)–(6.15) model the operation of the battery. Note that although the model registers every user transaction involving the battery (s_{jt}^{+}, s_{jt}^{-}), the cycles are constrained for the whole battery (i.e., the aggregated behavior of the $|J|$ users determines the battery use).

$$soc_{jt} = soc_{jt-1} + \frac{s_{jt}^{+} - s_{jt}^{-}}{S^{max}} \quad \forall \ j \in J, \ \forall \ t \in T \tag{6.12}$$

$$S^{max}(\alpha_t - 1) \leq \sum_{j \in J} (s_{jt}^{+} - s_{jt}^{-}) \leq S^{max} \alpha_t \quad \forall \ \ t \in T \tag{6.13}$$

$$-\alpha_t + \alpha_{t-1} \leq z_t \qquad \forall \;\; t \in T \tag{6.14}$$

$$\sum_{t \in T} z_t \leq Z \tag{6.15}$$

Constraint (6.12) updates the individual state of charge of each user. This value represents the amount of energy in the shared battery available to the user at every time step. Constraint (6.13) records the events when the battery (as a whole) charges or discharges. Constraints (6.14) and (6.15) limit the number of cycles. Note that these constraints do not differentiate between full and partial cycles. The parameter Z is a policy adopted by the building, and the optimization model will determine the type of cycle as a function of the cost and satisfaction. Section 6.4.4 shows how increasing Z affects the final number and type of cycles.

Solving a biobjective problem for the building does not mean that each user will profit in a similar way from the shared resources. Constraints (6.16) and (6.17) ensure a proportional use of the shared resources with respect to the total demand of each user.

$$\Psi_{sol}^{min} \sum_{t \in T} D_{jt} \leq \sum_{t \in T} g_{jt} \leq \Psi_{sol}^{max} \sum_{t \in T} D_{jt} \quad \forall \;\; j \in J \tag{6.16}$$

$$\Psi_{bat}^{min} \sum_{t \in T} D_{jt} \leq \sum_{t \in T} soc_{jt} \times S^{max} \leq \Psi_{bat}^{max} \sum_{t \in T} D_{jt} \quad \forall \;\; j \in J \tag{6.17}$$

Since $\sum_{t \in T} g_{jt} \leq \sum_{t \in T} D_{jt}$ (i.e., a housing unit cannot use more solar energy than its total demand), $\Psi_{sol}^{max} \leq 1$. An important assumption for the performance of the planning module is that the aggregated demand is always greater than the potential solar generation. This is justified by the building configuration: there are multiple housing units and limited space for roof-mounted panels. If we discarded this assumption, the optimization model could be adapted to absorb the excess solar generation into the battery or to sell it to the energy provider.

The parameter Ψ_{bat}^{max} has a different interpretation. The variable soc_{jt} tells us the level of energy in the battery for each user j and time frame t. For example, if the user charges 1 kWh at $t = 1$ and keeps it in the battery until $t = 10$, then $soc_{j1}, soc_{j2}, \ldots, soc_{j10}$ =1 kWh $/S^{max}$. The summation over these periods will be 10 kWh of *occupied* battery, regardless of the total demand. In this sense Ψ_{bat}^{max} can be > 1 but still represent fairness as a function of total demand (a user with larger demand can charge the battery with more energy or keep the battery busy for longer). The selection of the upper limits Ψ_{bat}^{max} and Ψ_{sol}^{max} must consider historical demand profiles and capacities to ensure proper utilization of the resources while

encouraging their fair allocation.

For the lower bounds Ψ_{bat}^{min} and Ψ_{sol}^{min} it is necessary to ensure feasibility, so they should satisfy

$$\Psi_{bat}^{min} \sum_{j \in J} \sum_{t \in T} D_{jt} \leq S^{max} \times |T|$$

and

$$\Psi_{sol}^{min} \sum_{j \in J} \sum_{t \in T} D_{jt} \leq \sum_{t \in T} G_t^{max}.$$

We discuss the fair allocation of resources in Section 6.4.5.

Constraints (6.18) and (6.19) account for the building response in the case of a DR request:

$$\sum_{j \in J} r_{jt} = DR_t \phi_t \quad \forall\ t \in T \tag{6.18}$$

$$x_{1jt} + x_{2jt} \leq (C^L + C_j^H)(1 - \phi_t) + D_{jt}\phi_t - r_{jt} \quad \forall\ j \in J, \forall\ t \in T \tag{6.19}$$

If the building agrees to provide DR, each user j will limit his/her consumption to the forecast demand. Additionally, the willing participants contribute r_{jt} units to the grid's load reduction requirement.

Constraint (6.19) allows the users to reduce their consumption below C^L. If $D_{jt} - r_{jt} \leq C^L$ the consumption will stay within the capacity available at a lower tariff. If $C_j^H + C^L \geq D_{jt} - r_{jt} \geq C^L$ the user will consume C^L units at the lower tariff and the additional energy at the higher tariff.

Finally, constraints (6.20) and (6.21) are the nonnegativity and binary constraints:

$$x, y, soc, s^+, s^-, g, r, \lambda \geq 0 \tag{6.20}$$

$$\alpha_t, z_t, \phi_t \in \{0, 1\}, \quad \forall \quad t \in T \tag{6.21}$$

6.3.4 Performance Measures

We use the peak reduction (PR) index and the battery use (BU) as measures of performance:

$$PR = \left(1 - \frac{\max\limits_{t \in T} \sum\limits_{i \in I} \sum\limits_{j \in J} x_{ijt}}{\max\limits_{t \in T} \sum\limits_{j \in J} D_{jt}}\right) \times 100\% \tag{6.22}$$

$$BU = \frac{\sum_{t \in T} \sum_{j \in J} soc_{jt}}{|T|} \times 100\% \tag{6.23}$$

Although these performance measures are not included in the optimization model, they are important assessments of the operation of the building, and they are reported for all our experiments. These measures could also be used to select efficient solutions in the case where we approximate the Pareto front.

6.4 Experimental Results

We carried out various tests to assess the impact of different conditions on the final results. In Section 6.4.1 we present a base instance (identified with $*$) to illustrate the results obtained with this approach. In subsequent sections we present the results of our sensitivity analysis. In Section 6.4.2 we explore how the peak reduction is affected by the parameters K_{it}, C^L, and C^H_j. In Section 6.4.3 we change the end-user willingness to shift load to see the evolution of the Pareto front and to estimate the expected consumer benefit of participating in this type of collaborative scheme. In Section 6.4.4 we analyze the relationship between the aggregated scheme and the operation of the battery and its cycles. Finally, in Section 6.4.5 we explore several options for the fair allocation of resources.

6.4.1 Base Instance

This instance, which has realistic parameters, includes the following conditions:

- The demand profiles D_{jt} are obtained from *Desimax* (Collin et al., 2014). Ten profiles ($|J| = 10$) were chosen for four-person households and were adjusted to the Canadian context, where heating represents around 60% of demand in winter (StatCan, 2013). The daily average energy consumption is 32.5 kWh.
- The battery capacity is $S^{max} = 15$ kWh, with a power capacity of 15 kW. The efficiency is $\Gamma = 90\%$, and the number of cycles is $Z = 2$. This battery is similar to the pole-mounted battery from *eCamion* in the context of the *NSERC Energy Storage Technology Network*. It is designed to facilitate the integration of energy management systems.
- There is a solar panel array of $75\,m^2$ with an average daily generation of 34.8 kWh, computed with an average solar radiation in winter of 3.45 kWh/m^2/day and a capacity

factor of 13.5% (NRE, 2016). The parameter G_t^{max} is accordingly defined with a peak generation of 4 kWh.

- While Y_j varies from user to user, $\hat{Y}_j = 0 \quad \forall j \in J$. The planning horizon has 24 time frames: $T = \{1, \ldots, 24\}$.
- The on-peak periods are $t \in \{8, 9, 10, 11, 17, 18, 19\}$, the mid-peak periods are $t \in \{12, \ldots, 16\}$, and the off-peak periods are $t \in \{1, \ldots, 7, 20, \ldots, 24\}$.
- There are six periods in which the building can meet a DR request of 10 kWh.
- The lower capacity $C^L = 1.5$ kW and

$$C_j^H = \max_{t \in T}(0, D_{jt} - C^L), \quad \forall \ \ j \in J. \tag{6.24}$$

This allows each user to consume up to the reported peak demand in any time frame. The initial values y_{j0}, soc_{j0}, and α_0 are 0.

Figure 6.3 shows the results for the base instance, obtained by solving the optimization model. Figure 6.3(a) shows that the consumption from the grid differs considerably from the original demand curve. A peak reduction of 13.9% ($t = 18$ on the blue curve versus $t = 20$ on the yellow curve) is achieved by a combination of solar resources, battery, and willingness to shift load. The battery is fully charged at $t = 7$ and $t = 16$, which are the time frames preceding the on-peak time frames. This generates a BU of 47.1%.

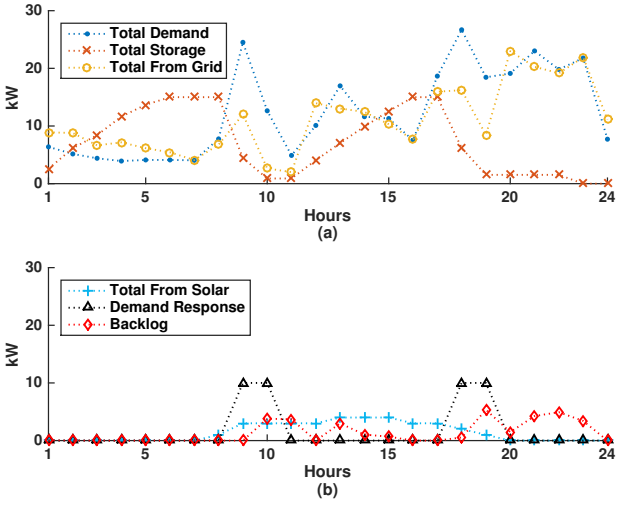

Figure 6.3 Results for the building in the base instance.

Figure 6.3(b) shows that the users willing to backlog demand make their contribution during the congested periods and consume their requirement by the end of the day. Additionally the building chooses to respond to 4 of 6 DR calls. We can see the reduction of 10 kW in time frames $9, 10, 18$, and 19, between the blue (total demand) and the yellow (total from grid) curves in Figure 6.3(a).

6.4.2 Cost Structure

The cost structure defined by K_{it}, B, and F determines some of the decisions made by the model. First, the cost F derived from the amortization of the solar panels should be lower than any price we can obtain from the grid. This renewable resource will be utilized first, leaving a net demand curve to be met by using the grid, storage, and load shifting.

As mentioned previously, K_{it}, C^L, and C^H_j are set by the building operator. Each time frame t belongs to one of three classes: on-peak, mid-peak, or off-peak. For each class the user pays either the *lower* or the *higher* cost, depending on the level of consumption. Figure 6.4 shows a basic representation of the TLOU pricing policy.

	Off-Peak	Mid-Peak	On-Peak
Higher	K_H^{off}	K_H^{mid}	K_H^{on}
Lower	K_L^{off}	K_L^{mid}	K_L^{on}

Figure 6.4 Energy cost structure.

We know that $K_H^{off} > K_L^{off}$, $K_H^{mid} > K_L^{mid}$, $K_H^{on} > K_L^{on}$, $K_L^{on} > K_L^{mid} > K_L^{off}$, and $K_H^{on} > K_H^{mid} > K_H^{off}$. In this section we establish some rules to determine how those costs can help to achieve the desired effect in the results. This analysis also includes the battery cost B, which we assume is obtained from cost amortization, and the willingness of the users to shift load.

Equations (6.25) and (6.26) show two possible cost structures for a cheaper and a more expensive period (off-peak and on-peak). The following reasoning can be extended to the other combinations: off-peak and mid-peak, and mid-peak and on-peak.

$$K_L^{off} + B < K_L^{on} < K_H^{off} + B < K_H^{on} \tag{6.25}$$

$$K_L^{off} + B < K_H^{off} + B < K_L^{on} < K_H^{on} \tag{6.26}$$

A cost structure based on equation (6.25) will encourage consumption of energy from the lower capacities before going to the higher level. On the other hand, a cost structure based on equation (6.26) will encourage using all the off-peak resources before moving to more expensive time frames.

The selection of the cost structure is key for the decision making in two specific circumstances:

1. The user shifts load from the on-peak to the future off-peak periods. In this case the battery cost is not included (i.e., $B = 0$).

2. The user wants to charge the battery in the off-peak time frames to use the energy in the later on-peak periods. Here the battery cost $B > 0$ is considered.

Table 6.1 reports the results for both cost structures. The parameter C^L increases by 0.5 kWh from one instance to the next.

Table 6.1 Comparison of cost structures and available capacities

Inst	K_{it}	C^L	f_1	f_2	PR	BU
1	(6.25)	1.0	31.0	2973.9	−0.8	44.7
2*	(6.25)	1.5	32.2	2750.4	13.9	47.1
3	(6.25)	2.0	33.7	2615.0	10.2	47.1
4	(6.25)	2.5	33.4	2535.3	−1.6	49.1
5	(6.26)	1.0	34.6	2703.4	−46.5	42.9
6	(6.26)	1.5	34.6	2605.6	−25.7	47.1
7	(6.26)	2.0	34.0	2543.3	−10.6	47.1
8	(6.26)	2.5	34.0	2499.8	−17.5	43.8

First, observe that the BU is similar in every case; it depends on the capacity of the battery and the number of time frames where using the battery makes sense.

Observe also that the instances with equation (6.25) report a better PR. In fact, the peak demand *increases* considerably for the instances with equation (6.26). In general terms, equation (6.25) leads to a more homogeneous use of the available capacities, where energy is first consumed in the lower levels regardless of the time of use.

Of the experiments with equation (6.25), instances 2* and 3 achieve better PR; the peak slightly increases in instances 1 and 4. A low C^L will be consumed quickly and the shiftable

demand will accumulate in the higher level of the cheapest time frames. A large C^L will render the higher level useless and will accumulate the shiftable demand in the lower level of the cheapest time frames. In both cases we basically move the peak from an expensive period to a cheaper one. Figure 6.5 shows the peak reduction as a function of C^L using the costs in (6.25). We see that the PR is positive for only a small range of C^L, approximately 1.1 to 2.4.

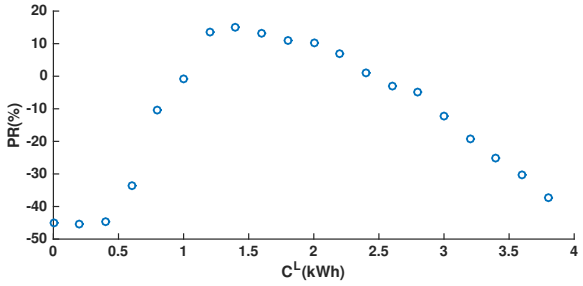

Figure 6.5 Peak reduction as a function of C^L.

It is important to recall that PR is not considered in the optimization problem, and our approach achieves the PR as an additional effect. Nevertheless, our discussion can guide future decisions about how to determine the capacity profiles.

6.4.3 Willingness to Participate

In this section we show how the end-user willingness to shift load affects the results. We change the parameter Y_j in each instance in Table 6.2. In instance 1 the users are more willing to shift load, and in instance 5 the users prefer not to change their consumption patterns.

Table 6.2 Results for different populations

Inst	$\tilde{u_1}$	$\tilde{u_2}$	f_1	f_2	PR	BU	Φ
1	0.0	2632.1	51.0	2703.5	17.2	47.1	4/6
2*	0.0	2678.2	32.2	2750.4	13.9	47.1	4/6
3	0.0	2774.2	10.1	2816.4	14.6	46.8	4/6
4	0.0	2838.1	3.2	2854.4	16.4	49.7	3/6
5	0.0	2873.2	0.5	2876.0	13.7	46.5	2/6

The utopian value $\tilde{u_1}$ remains the same while $\tilde{u_2}$ increases as the willingness to shift load

reduces. The compromise solution (f_1, f_2) becomes closer to the utopia point. The evolution of the Pareto front is shown in Figure 6.6.

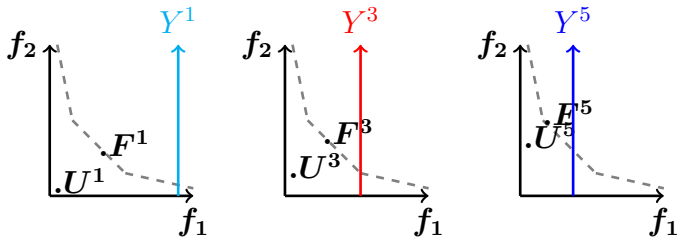

Figure 6.6 Evolution of the Pareto front.

Y^{inst}, F^{inst}, and U^{inst} represent the aggregated willingness, the compromise solution, and the utopia point for each instance respectively. The BU has similar behavior to that in Section 6.4.2.

Although we achieve PR in all the instances, the behavior with respect to Y_j is not clear: Y_j can generate a higher or lower PR depending on the selection of C^L and the prices.

In the last column we introduce the ratio Φ, which is defined to be the total number of DR calls accepted by the building divided by the potential DR requests. As the willingness to shift load decreases the building responds to fewer DR requests.

Table 6.3 gives the individual cost per user and instance. Typically, the more willing the user is to shift load the lower the total cost. In the last column we compute the total cost for a scenario Ω without the collaborative approach. In this case there are no resources (storage, solar panels, or DR incentives). The users meet their demands as they occur, paying the same cost rates K_{it}.

Table 6.3 Total cost per housing unit

User	Inst1	Inst2	Inst3	Inst4	Inst5	Ω
1	177.4	179.9	181.3	183.1	183.1	211.6
2	328.6	341.7	352.3	363.9	357.8	446.5
3	278.0	286.6	308.3	282.7	284.0	453.9
4	301.4	305.6	309.8	315.4	323.0	412.8
5	203.6	206.6	210.0	213.0	213.0	251.3
6	384.9	383.3	427.2	422.5	433.6	529.4
7	216.1	216.7	218.2	223.4	223.1	276.2
8	270.8	271.8	251.8	288.3	296.4	357.4
9	238.0	248.4	247.7	248.0	248.0	278.8
10	304.8	309.9	310.0	314.2	314.0	369.0

One of the key assumptions of this work is that the parameters B and F, representing the amortization costs of the battery and the solar panels, must be lower than the rates that come from the grid or the building operator. Therefore, the collaboration allows the user to take advantage of resources that would be more expensive to own individually. In general terms, the more willing the user is to shift load, the lower the total cost will be. However, this statement is not necessarily true. A willing user may not be asked to shift load; this depends on the global benefit that the shifting provides to the community (because the model gives priority to users that can shift load from on-peak periods).

6.4.4 Battery Cycles and Aggregation

One of the most common issues with storage units is the proper use of the resource to minimize its degradation. Although in this paper we assume an amortization cost to take this into account, we also included constraints to control the number of cycles. The results for different values of Z are presented in Table 6.4.

Table 6.4 Results for different maximum number of cycles

Inst	u_1	u_2	f_1	f_2	PR	BU	z/Z
1	0.0	2708.6	35.1	2789.3	13.9	52.7	1/1
2*	0.0	2678.2	32.2	2750.4	13.9	47.1	2/2
3	0.0	2678.2	32.1	2750.4	13.9	47.1	3/3
4	0.0	2678.2	32.1	2750.4	13.9	47.1	3/6
5	0.0	2678.2	32.1	2750.4	13.9	47.1	3/12

We observe that the number of cycles is fairly stable at $z = 3$, giving the same compromise solution regardless of the value of Z. What happens is that the number of cycles is determined by the cost structure in combination with the user demand. There are only some periods where it is sensible to use the battery: charge in the current (cheaper) frame to discharge in a future (more expensive) one.

6.4.5 Allocation of Resources

In Section 6.3.3 we introduced the fair allocation of the shared resources with constraints (6.16) and (6.17). In this section we assess the effect of this on the objective function. We test three models (the original and two variations). In the first we do not include a fairness constraint; in the second we include the original constraints (6.16) and (6.17); and in the third we include constraints (6.27) and (6.28) instead:

$$\sum_{t \in T} g_{jt} - \sum_{t \in T} g_{j-1t} = 0 \qquad \forall \;\; j \in J \mid j > 1 \tag{6.27}$$

$$\sum_{t \in T} soc_{jt} - \sum_{t \in T} soc_{j-1t} = 0 \qquad \forall \;\; j \in J \mid j > 1 \tag{6.28}$$

Constraint (6.27) ensures that all the users obtain the same amount of energy from the solar panels. In a similar way, constraint (6.28) ensures that all the users have the same accumulated state of charge over the time horizon (i.e., the battery is equally utilized). We report the results in Table 6.5. Model 1 gives the lowest cost but does not ensure a fair distribution of the resources; model 3 gives the lowest shifted load.

Table 6.5 Results for different fairness constraints

Variation	f_1	f_2
1	34.7	2727.6
2*	32.2	2750.4
3	31.3	2774.7

Figure 6.7 presents more detailed results for each user. Figure 6.7(a) shows the solar allocation expressed as a percentage of the demand ($\sum_{t\in T} g_{jt} / \sum_{t\in T} D_{jt}$). Figure 6.7(b) shows the battery allocation ($\sum_{t\in T} soc_{jt} \times S^{max} / \sum_{t\in T} D_{jt}$), and Figure 6.7(c) gives the shifted load as a percentage of the total shiftable load ($\sum_{t\in T} y_{jt} / Y_j$).

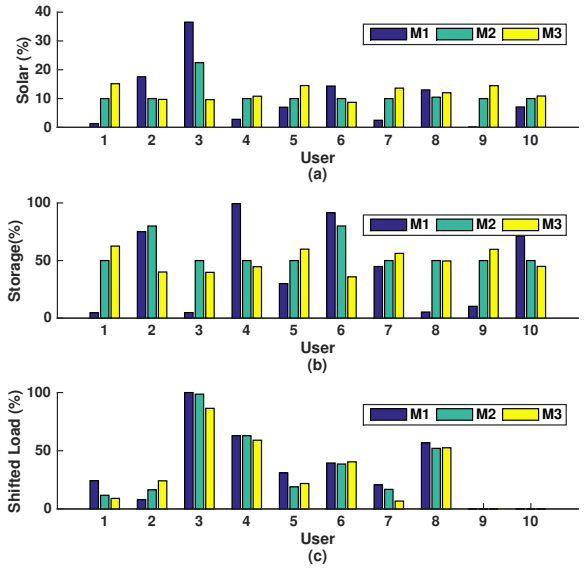

Figure 6.7 Comparison of allocation of resources per user. Solar and battery are expressed as a percentage of the demand, and shifted load is expressed as a percentage of the total shiftable load.

Model 1 (blue bars) varies considerably from user to user in Figures 6.7(a) and (b). Models 2 and 3 give similar variations among the users. In this particular case the set of realistic demands D_{jt} can have high variation, which makes it suboptimal to force the same utilization for each user (as in model 3). Whether or not model 2 is better than model 3 also depends on the selection of the parameters Ψ_{bat}^{max}, Ψ_{sol}^{max}, Ψ_{bat}^{min}, and Ψ_{sol}^{min}.

Finally, in Figure 6.7(c) we see a similar shifted load per user. Model 1 compensates for the

lack of battery utilization of users 3, 5, and 8 by increasing their shifted load. This gives a fairer allocation without a significant deterioration in the performance.

6.5 Conclusion

The approach presented in this work contributes to the planning and operation of smart buildings. It has a structure similar to that of classic LS, but it supports decision-making in the context of energy consumption for a multi-unit building. We address two conflicting objectives, cost and comfort, via the compromise solution. The proposed approach balances the two objectives while providing demand response to the grid. This is possible because of the combination of the available resources (solar and storage), active user participation, and a cost structure that provides incentives for load shifting and peak reduction.

We presented a detailed analysis of the effect of the different parameters on the compromise solution. This analysis provides insights into the conditions needed to ensure the long-term operation and economic viability of the approach for the building and the individual users.

Acknowledgments

This research was supported by the Canada Research Chair on Discrete Nonlinear Optimization in Engineering and by the NSERC Energy Storage Technology Network.

CHAPTER 7 CONCLUDING REMARKS

7.1 General Discussion

There is an an intuitive connection among the contributions although they have different components. There are different approaches for different types of loads, and similar decisions can be made at an aggregated level. The main features are listed in Table 7.1.

Table 7.1 Summary of the contributions

Article	Demand satisfaction	Cost	Granularity	Capacity profile
1 (Thermal)	QoS defined by user	not considered	unit ← load	QoS function
2 (Activity)	100%	minimized	unit ← load	cost function
3 (Planning)	Shifting limited by user	traded-off	building ← unit	set by utility

The first two contributions have the same granularity, obtaining information from individual loads and making decisions for a single housing unit. In both cases, the user determines the capacity required. The main differences are the load types and the decision criteria. The thermal loads could be treated as activity loads, assuming that the external temperature is a stochastic parameter and that the user books capacity for a longer period (e.g., weekly or monthly). In this scenario the first contribution could help to *translate* the external temperature into capacity requirements, and the second contribution would handle these requirements as activity loads that arrive depending on the external temperature.

The third contribution makes decisions at a higher level given the demand and shifting preference information obtained from the lower levels. This module takes an initial demand curve per housing unit, computes a Pareto-optimal solution for the building, and returns a new demand curve (net demand) to each user. Conceptually, these new demand profiles can be seen as limits imposed on the users (i.e., capacity profiles) that will guide the consumption and operation of the individual loads at the housing-unit level. It will be necessary to coordinate the decisions made at the household level and those made at the building level to guarantee the correct operation and the expected user satisfaction. The adjustments include a unified measure of level of service and the tariff setting (defined by the grid, the building, or both). Some of these will be explored in Section 7.3.

7.2 Limitations

In general terms, the continuous requirement for quality information is present throughout this thesis. The data flow from appliances and other devices towards higher levels is a strong condition that supports all the work presented here.

We discussed in Section 4.3 the importance of proper calibration between the QoS and the interval of operation in each room. Although the QoS index allows us to aggregate several thermal devices and their dynamics, it must represent the actual comfort experienced by the users. Additionally, this method could be considered static since the training, fitting, and classification process is carried out for only one home configuration. If a modification is made to the smart home such as an improvement to the efficiency of the insulation, heaters or air conditioners, the estimation process must be repeated. One of the main advantages of using the QoS is that it facilitates scalability. For the fifty-heater instance, the approach determines the required capacity profile in seconds. On the other hand, the QoS is a system performance measure that may not be properly understood by the user. In this case, the users must directly manage the desired temperature, and the system derives the desired QoS from that information.

For the stochastic optimization in Chapter 5, there are two main challenges: time scale and scenario elimination. The time-scale selection is important since the durations of appliance use are continuous values ranging from minutes to hours. The combination of a large number of loads leads to an exponential growth of the potential scenarios, so the elimination of non-significant scenarios may have an impact on the optimal solution. It is necessary to find an appropriate time scale and number of scenarios to provide sufficient information while keeping the solution time under control. This will allow proper scalability.

Since cost was considered in Chapter 6 as one of the two objectives, this approach is applicable only to jurisdictions where time-based pricing and/or incentive based DR programs exist. Without these, the decision becomes trivial, since the use of the battery increases the total cost, there are no shifting-related incentives, and the best approach is simply to absorb the energy generated by the solar panels and to draw the net demand directly from the grid. DR programs allow us to trade-off cost and demand satisfaction while contributing to peak reduction. This effect was enhanced in Section 6.4 by the use of the solar panels and battery. These two technologies are assumed to be mature enough to provide cost-effective solutions that are competitive with the energy tariffs offered by the utility or grid operator.

With respect to scalability, the model can be solved for larger instances with the available solvers. This introduces a more conceptual discussion about whether a full centralized plan-

ning approach is a realistic strategy for larger populations.

In addition to the technical limitations, there is the challenge of successful implementation. Social acceptance is one of the most important aspects in the evolution of SGs since the paradigm shifting leads to new questions for users. Several barriers to implementation have been identified for DR programs (Weck et al., 2017). In particular, the uncertainty related to the global economic benefit for the users seems to affect the ability to attract participants. The reward may be insufficient to encourage DR. The flexible TLOU seeks to provide users with appropriate energy prices. However, these prices must take grid performance into account and ensure that the grid remains economically feasible.

The acceptance of solar generation and storage technologies can vary from strong opposition to smooth integration (Upham et al., 2015). Sharing these resources among multiple users can reduce both cost and other acceptance barriers such as space allocation and risk aversion.

7.3 Future Work

The most immediate future work concerns the integration of the user capacity estimation and the building planning modules, and the price setting at the grid level given a population of consumption-aware users. Figure 7.1 shows how these ideas would fit into this research project. It shows each of the contributions of this thesis, with future projects shown in boxes and denoted A, B and C. The current and future projects are connected by dashed red lines.

As mentioned previously, the second contribution in Chapter 5 ensures that the total user demand is satisfied and allows savings via a flexible tariff structure. In some cases, the characteristics of the user behavior (i.e., the expected demand) may not lead to any benefit from the proposed tariff structure. The optimal solution is then to book zero capacity.

In project A the user could adapt some preferences so that the expected demand will grant better savings. A scheduling module is required to guide users when the potential savings are significant compared to the loss of satisfaction or comfort in a given period. The expected demand would change from a consumption based on preferences to an optimized consumption.

In the third contribution the decisions are made at the building level and the information is passed to the users. Project B accounts for this transition by using a scheduling module to fit the appliance consumption to a consumption curve determined by the building planning module.

Although the scheduler module could be the same for A and B, the goals are different. In the case of A, the users want to improve their savings while in B, the users react to a condition imposed from a *dictator* perspective.

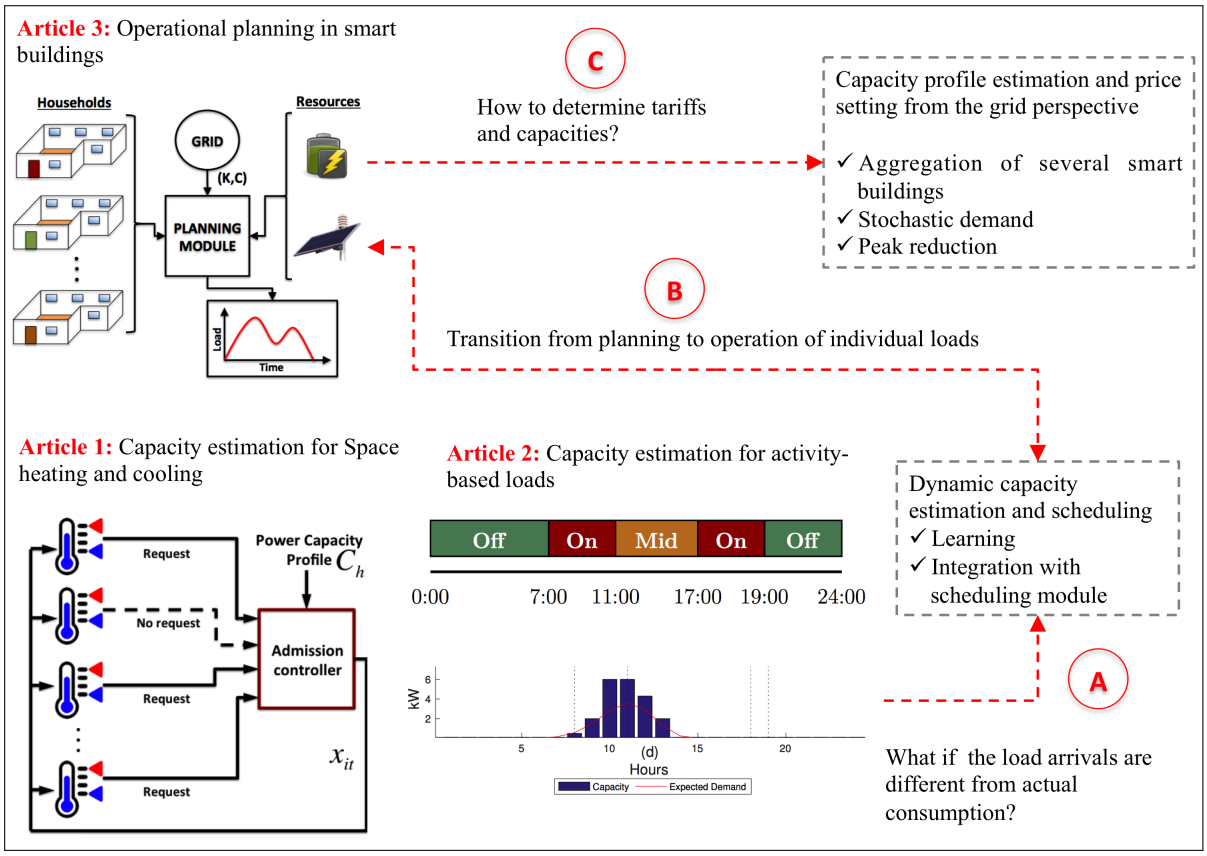

Figure 7.1 Current and future work on user-oriented DR for smart buildings

Finally, project C would consider at the grid level the decisions made locally in each building. This specifically refers to the situation introduced in Section 6.4.2, where different configurations of TLOU with different capacities could lead to an increase in the peak demand. From a grid perspective, setting the tariff structure and the capacity limit is key to ensuring the performance of the system. At this level, it is necessary to consider multiple buildings, stochastic demands, and in general an equilibrium between the utility profit and the effect of the prices on the demand. This creates the potential need for intermediate aggregation levels that facilitate the transition from a single building to a network-oriented perspective.

7.4 Conclusions

This thesis proposes a framework for facilitating and encouraging end-user participation in DR programs. We considered different features while focusing on the user perspective. These approaches explore the current characteristics of smart building operation and take a step towards the integration of user-oriented tools.

This framework addresses three conflicting goals: user satisfaction, user cost, and peak control. We prioritize demand satisfaction, but we provide a balance among the conflicting goals through an appropriate combination of resources such as solar panels, battery, tariffs, and the admission controller.

Enhanced user participation will contribute to the continued evolution of power systems, increasing the flexibility, reliability, and stability of this key resource.

BIBLIOGRAPHY

S. Afsar, L. Brotcorne, P. Marcotte, and G. Savard, "Achieving an optimal trade-off between revenue and energy peak within a smart grid environment," *Renewable Energy*, vol. 91, pp. 293–301, 2016.

J. Aghaei and M.-I. Alizadeh, "Multi-objective self-scheduling of CHP (combined heat and power)-based microgrids considering demand response programs and ESSs (energy storage systems)," *Energy*, vol. 55, pp. 1044–1054, 2013.

K. Ahmed, M. Ampatzis, P. Nguyen, and W. Kling, "Application of time-series and artificial neural network models in short term load forecasting for scheduling of storage devices," in *Power Engineering Conference (UPEC), 2014 49th International Universities*, Sept 2014, pp. 1–6.

A. Al-Wakeel, J. Wu, and N. Jenkins, "k-means based load estimation of domestic smart meter measurements," *Applied Energy*, vol. 194, pp. 333–342, 2017.

T. AlSkaif, A. C. Luna, M. G. Zapata, J. M. Guerrero, and B. Bellalta, "Reputation-based joint scheduling of households appliances and storage in a microgrid with a shared battery," *Energy and Buildings*, vol. 138, pp. 228–239, 2017.

J. R. Birge and F. Louveaux, *Introduction to Stochastic Programming*. Springer Science & Business Media, 2011.

X. Cao, J. Wang, and Z. Zhang, "Multi-objective optimization of preplanned microgrid islanding based on stochastic short-term simulation," *International Transactions on Electrical Energy Systems*, vol. 27, no. 1, 2017.

P. Cappers, C. Goldman, and D. Kathan, "Demand response in U.S. electricity markets: Empirical evidence," *Energy*, vol. 35, no. 4, pp. 1526–1535, 2010.

D. Caprino, M. L. D. Vedova, and T. Facchinetti, "Peak shaving through real-time scheduling of household appliances," *Energy and Buildings*, vol. 75, pp. 133–148, 2014.

A. Chabaud, J. Eynard, and S. Grieu, "A new approach to energy resources management in a grid-connected building equipped with energy production and storage systems: A case study in the south of France," *Energy and Buildings*, vol. 99, pp. 9–31, 2015.

N. V. Chawla, "Data mining for imbalanced datasets: An overview," in *The Data Mining and Knowledge Discovery Handbook*, O. Maimon and L. Rokach, Eds. Springer US, 2005, pp. 875–886.

Z. Chen, L. Wu, and Y. Fu, "Real-time price-based demand response management for residential appliances via stochastic optimization and robust optimization," *IEEE Transactions on Smart Grid*, vol. 3, no. 4, pp. 1822–1831, Dec 2012.

M. Choobineh and S. Mohagheghi, "A multi-objective optimization framework for energy and asset management in an industrial microgrid," *Journal of Cleaner Production*, vol. 139, pp. 1326–1338, 2016.

Climate, "Historical climate data," http://climate.weather.gc.ca, 2016, [Goverment of Canada; accessed July 2016].

D. Cluwen, "Demand response and storage for demand side management in smart buildings," University of Twente and Polytechnique Montreal, Internship Report, April 2014.

A. J. Collin, G. Tsagarakis, A. E. Kiprakis, and S. McLaughlin, "Development of low-voltage load models for the residential load sector," *IEEE Transactions on Power Systems*, vol. 29, no. 5, pp. 2180–2188, Sept 2014.

G. T. Costanzo, G. Zhu, M. F. Anjos, and G. Savard, "A system architecture for autonomous demand side load management in smart buildings," *IEEE Transactions on Smart Grid*, vol. 3, no. 4, pp. 2157–2165, 2012.

K. P. Detroja, "Optimal autonomous microgrid operation: A holistic view," *Applied Energy*, vol. 173, pp. 320–330, 2016.

R. Diao, S. Lu, M. Elizondo, E. Mayhorn, Y. Zhang, and N. Samaan, "Electric water heater modeling and control strategies for demand response," in *2012 IEEE Power and Energy Society General Meeting*, July 2012, pp. 1–8.

T. E. Dielman, "A comparison of forecasts from least absolute value and least squares regression," *Journal of Forecasting*, vol. 5, no. 3, pp. 189–195, 1986.

G. L. Doorman, "Capacity subscription: Solving the peak demand challenge in electricity markets," *IEEE Transactions on Power Systems*, vol. 20, no. 1, pp. 239–245, Feb 2005.

M. Ehrgott, *Multicriteria Optimization*. Springer Science & Business Media, 2006.

EIA, “Electric Power Annual 2014,” U.S. Energy Information Administration, Tech. Rep., 2016.

B. P. Esther and K. S. Kumar, “A survey on residential demand side management architecture, approaches, optimization models and methods,” *Renewable and Sustainable Energy Reviews*, vol. 59, pp. 342–351, 2016. [Online]. Available: http://www.sciencedirect.com/science/article/pii/S1364032115016652

FERC, “Assessment of Demand Response and Advanced Metering,” Federal Energy Regulatory Commission, Tech. Rep., 2012.

F. Fernandes, H. Morais, Z. Vale, and C. Ramos, “Dynamic load management in a smart home to participate in demand response events,” *Energy and Buildings*, vol. 82, pp. 592–606, 2014.

C. W. Gellings, “The concept of demand-side management for electric utilities,” *Proceedings of the IEEE*, vol. 73, no. 10, pp. 1468–1470, Oct 1985.

J. A. Gomez and M. F. Anjos, “Power capacity profile estimation for building heating and cooling in demand-side management,” *Applied Energy*, vol. 191, pp. 492–501, 2017.

——, “Collaborative demand-response planner for smart buildings,” *Les Cahiers du Gerad*, March 2017.

A. A. Hasib, N. Nikitin, and L. Natvig, “Cost-comfort balancing in a smart residential building with bidirectional energy trading,” in *2015 Sustainable Internet and ICT for Sustainability (SustainIT)*, April 2015, pp. 1–6.

V. Hosseinnezhad, M. Rafiee, M. Ahmadian, and P. Siano, “Optimal day-ahead operational planning of microgrids,” *Energy Conversion and Management*, vol. 126, pp. 142–157, 2016.

Hydro-Quebec, “Electricity rates 2017,” Hydro Quebec, Tech. Rep., 2017.

IESO, “2014 Yearbook of Electricity Distributors,” Ontario Energy Board, Tech. Rep., 2015.

R. K. Jain, K. M. Smith, P. J. Culligan, and J. E. Taylor, “Forecasting energy consumption of multi-family residential buildings using support vector regression: Investigating the impact of temporal and spatial monitoring granularity on performance accuracy,” *Applied Energy*, vol. 123, pp. 168–178, 2014.

C. D. Korkas, S. Baldi, I. Michailidis, and E. B. Kosmatopoulos, “Occupancy-based demand response and thermal comfort optimization in microgrids with renewable energy sources and energy storage,” *Applied Energy*, vol. 163, pp. 93–104, 2016.

P. O. Kriett and M. Salani, "Optimal control of a residential microgrid," *Energy*, vol. 42, no. 1, pp. 321–330, 2012.

M. Kuzlu, M. Pipattanasomporn, and S. Rahman, "Hardware demonstration of a home energy management system for demand response applications," *IEEE Transactions on Smart Grid*, vol. 3, no. 4, pp. 1704–1711, Dec 2012.

X. Li, H. H. Chen, and X. Tao, "Pricing and capacity allocation in renewable energy," *Applied Energy*, vol. 179, pp. 1097–1105, 2016.

T. Logenthiran, D. Srinivasan, and T. Z. Shun, "Demand side management in smart grid using heuristic optimization," *IEEE Transactions on Smart Grid*, vol. 3, no. 3, pp. 1244–1252, Sept 2012.

J. M. Lujano-Rojas, C. Monteiro, R. Dufo-López, and J. L. Bernal-Agustín, "Optimum residential load management strategy for real time pricing (RTP) demand response programs," *Energy Policy*, vol. 45, pp. 671–679, 2012.

K. Margellos and S. Oren, "Capacity controlled demand side management: A stochastic pricing analysis," *IEEE Transactions on Power Systems*, vol. 31, no. 1, pp. 706–717, 2016.

R. T. Marler and J. S. Arora, "Survey of multi-objective optimization methods for engineering," *Structural and Multidisciplinary Optimization*, vol. 26, no. 6, pp. 369–395, 2004.

J. Massana, C. Pous, L. Burgas, J. Melendez, and J. Colomer, "Short-term load forecasting in a non-residential building contrasting models and attributes," *Energy and Buildings*, vol. 92, pp. 322–330, 2015.

P. Mesari and S. Krajcar, "Home demand side management integrated with electric vehicles and renewable energy sources," *Energy and Buildings*, vol. 108, pp. 1–9, 2015.

S. Mhanna, A. C. Chapman, and G. Verbič, "A fast distributed algorithm for large-scale demand response aggregation," *IEEE Transactions on Smart Grid*, vol. 7, no. 4, pp. 2094–2107, July 2016.

S. Mohajeryami, M. Doostan, A. Asadinejad, and P. Schwarz, "Error analysis of customer baseline load calculation methods for residential customers," *IEEE Transactions on Industry Applications*, vol. 53, no. 1, pp. 5–14, 2017.

S. Moon and J. W. Lee, "Multi-residential demand response scheduling with multi-class appliances in smart grid," *IEEE Transactions on Smart Grid*, vol. PP, no. 99, pp. 1–1, 2016.

J. Munkhammar, J. Ryden, and J. Widen, "Characterizing probability density distributions for household electricity load profiles from high-resolution electricity use data," *Applied Energy*, vol. 135, pp. 382–390, 2014.

M. Muratori and G. Rizzoni, "Residential demand response: Dynamic energy management and time-varying electricity pricing," *IEEE Transactions on Power Systems*, vol. 31, no. 2, pp. 1108–1117, March 2016.

T. A. Nguyen and M. Aiello, "Energy intelligent buildings based on user activity: A survey," *Energy and Buildings*, vol. 56, pp. 244–257, 2013.

NRCan, "Survey of Household Energy Use," Natural Resources Canada, Tech. Rep., 2011.

NRE, "Pvwatts calculator," National Renewable Energy Laboratory, Tech. Rep., 2016.

A. Ogunjuyigbe, T. Ayodele, and O. Akinola, "User satisfaction-induced demand side load management in residential buildings with user budget constraint," *Applied Energy*, vol. 187, pp. 352–366, 2017.

B. Olesen and K. Parsons, "Introduction to thermal comfort standards and to the proposed new version of EN ISO 7730," *Energy and Buildings*, vol. 34, no. 6, pp. 537–548, 2002.

R. Palma-Behnke, C. Benavides, F. Lanas, B. Severino, L. Reyes, J. Llanos, and D. Saez, "A microgrid energy management system based on the rolling horizon strategy," *IEEE Transactions on Smart Grid*, vol. 4, no. 2, pp. 996–1006, 2013.

S. Parhizi, H. Lotfi, A. Khodaei, and S. Bahramirad, "State of the art in research on microgrids: A review," *IEEE Access*, vol. 3, pp. 890–925, 2015.

A. Parisio, E. Rikos, and L. Glielmo, "A model predictive control approach to microgrid operation optimization," *IEEE Transactions on Control Systems Technology*, vol. 22, no. 5, pp. 1813–1827, Sept 2014.

Y. Pochet and L. A. Wolsey, *Production Planning by Mixed Integer Programming*. Springer Science & Business Media, 2006.

S. Rahim, N. Javaid, A. Ahmad, S. A. Khan, Z. A. Khan, N. Alrajeh, and U. Qasim, "Exploiting heuristic algorithms to efficiently utilize energy management controllers with renewable energy sources," *Energy and Buildings*, vol. 129, pp. 452–470, 2016.

M. Rastegar, M. Fotuhi-Firuzabad, and H. Zareipour, "Home energy management incorporating operational priority of appliances," *International Journal of Electrical Power & Energy Systems*, vol. 74, pp. 286–292, 2016.

I. Richardson, M. Thomson, D. Infield, and C. Clifford, "Domestic electricity use: A high-resolution energy demand model," *Energy and Buildings*, vol. 42, no. 10, pp. 1878–1887, 2010.

SEN, "Condizioni di fornitura," Servizio Elettrico Nazionale, Tech. Rep., 2017.

P. Siano, "Demand response and smart grids: A survey," *Renewable and Sustainable Energy Reviews*, vol. 30, pp. 461–478, 2014.

A. Soares, A. Gomes, and C. H. Antunes, "Categorization of residential electricity consumption as a basis for the assessment of the impacts of demand response actions," *Renewable and Sustainable Energy Reviews*, vol. 30, pp. 490–503, 2014.

StatCan, "Households and the Environment: Energy Use," http://www.statcan.gc.ca/pub/11-526-s/11-526-s2013002-eng.htm, Statistics Canada, Tech. Rep., 2013.

R. Subbiah, K. Lum, A. Marathe, and M. Marathe, "Activity based energy demand modeling for residential buildings," in *Innovative Smart Grid Technologies (ISGT), 2013 IEEE PES*, Feb 2013, pp. 1–6.

L. Suganthi and A. A. Samuel, "Energy models for demand forecasting: A review," *Renewable and Sustainable Energy Reviews*, vol. 16, no. 2, pp. 1223–1240, 2012.

L. G. Swan and V. I. Ugursal, "Modeling of end-use energy consumption in the residential sector: A review of modeling techniques," *Renewable and Sustainable Energy Reviews*, vol. 13, no. 8, pp. 1819–1835, 2009.

P. Upham, C. Oltra, and A. Boso, "Towards a cross-paradigmatic framework of the social acceptance of energy systems," *Energy Research and Social Science*, vol. 8, pp. 100–112, 2015.

J. S. Vardakas, N. Zorba, and C. V. Verikoukis, "A survey on demand response programs in smart grids: Pricing methods and optimization algorithms," *IEEE Communications Surveys Tutorials*, vol. 17, no. 1, pp. 152–178, 2015.

R. Walawalkar, S. Fernands, N. Thakur, and K. R. Chevva, "Evolution and current status of demand response (DR) in electricity markets: Insights from PJM and NYISO," *Energy*, vol. 35, no. 4, pp. 1553–1560, 2010.

M. Weck, J. Hooff, and W. Sark, "Review of barriers to the introduction of residential demand response: A case study in the Netherlands," *International Journal of Energy Research*, vol. 41, no. 6, pp. 790–816, 2017.

R. Yang and L. Wang, "Multi-objective optimization for decision-making of energy and comfort management in building automation and control," *Sustainable Cities and Society*, vol. 2, no. 1, pp. 1–7, 2012.

H. Zareipour, D. Huang, and W. Rosehart, "Wind power ramp events classification and forecasting: A data mining approach," in *2011 IEEE Power and Energy Society General Meeting*, July 2011, pp. 1–3.

H. Zareipour, A. Janjani, H. Leung, A. Motamedi, and A. Schellenberg, "Classification of future electricity market prices," *IEEE Transactions on Power Systems*, vol. 26, no. 1, pp. 165–173, Feb 2011.

X. Zhang, R. Sharma, and Y. He, "Optimal energy management of a rural microgrid system using multi-objective optimization," in *2012 IEEE PES Innovative Smart Grid Technologies (ISGT)*, Jan 2012, pp. 1–8.